

# **FFI RAPPORT**

**BROADBAND INVERSION AND SOURCE  
LOCALIZATION OF VERTICAL ARRAY DATA  
FROM THE L-ANTENNA EXPERIMENT IN  
1999**

EIDEM Ellen Johanne

**FFI/ RAPPORT- 2002/ 02565**



FFIBM/786/115

Approved  
Horten 28. June 2002

Jarl Johnsen  
Director of Research

**BROADBAND INVERSION AND SOURCE  
LOCALIZATION OF VERTICAL ARRAY DATA  
FROM THE L-ANTENNA EXPERIMENT IN 1999**

EIDEM Ellen Johanne

FFI/RAPPORT-2002/02565

**FORSVARETS FORSKNINGSINSTITUTT  
Norwegian Defence Research Establishment  
P O Box 25, NO-2027 Kjeller, Norway**



**FORSVARETS FORSKNINGSIINSTITUTT (FFI)**  
**Norwegian Defence Research Establishment**

**UNCLASSIFIED**

P O BOX 25  
 NO-2027 KJELLER, NORWAY  
**REPORT DOCUMENTATION PAGE**

**SECURITY CLASSIFICATION OF THIS PAGE  
 (when data entered)**

1) PUBL/ REPORT NUMBER  FFI/RAPPORT-2002/02565	2) SECURITY CLASSIFICATION  UNCLASSIFIED	3) NUMBER OF PAGES  49
1a) PROJECT REFERENCE  FFIBM/786/115	2a) DECLASSIFICATION/ DOWNGRADING SCHEDULE  -	
4) TITLE  BROADBAND INVERSION AND SOURCE LOCALIZATION OF VERTICAL ARRAY DATA FROM THE L-ANTENNA EXPERIMENT IN 1999		
5) NAMES OF AUTHOR(S) IN FULL (surname first)  EIDEM Ellen Johanne		
6) DISTRIBUTION STATEMENT  Approved for public release. Distribution unlimited. (Offentlig tilgjengelig)		
7) INDEXING TERMS IN ENGLISH:		IN NORWEGIAN:
a) Matched field processing	b) Localization	c) Geoacoustic properties
d) Broadband	e) Shallow water	f) Mediatilpasset signalbehandling
		g) Lokalisering
		h) Geoakustiske egenskaper
		i) Bredbånd
		j) Grunt vann
THESSAURUS REFERENCE:		
8) ABSTRACT  Matched field processing techniques have been demonstrated on vertical array data from the 1999 L-antenna experiment. Both single-frequency and broadband inversion of geoacoustic and geometric parameters were carried out. The baseline model consisted of three water layers and a sediment layer overlying a half-space substrate. The environment was assumed range-independent with no shear waves. Broadband inversion showed to be more robust than single-frequency inversion. For broadband inversion the estimate of the water depth was usually between the depths at receiver and source positions. The p-wave sound velocity in the sediment was estimated to be about 1600 m/s, which was 200 m/s lower than in the baseline model. The sediment thickness was estimated to be thicker than in the baseline model, which conflicted with the measured two-way travel time.  Broadband source localization (range and depth) showed to be most successful when using a modified baseline model and at the same time inverting the water depth. The error in the range estimate was only 1 – 6 %, while the error in the depth estimate was 4 – 16 %. The depth was underestimated for the 91 m and 244 m shots, and usually overestimated for the 18 m shots. The range was usually underestimated. The best matches in both inversion and localization were found for the 18 m shots. The OASES module OAST and SAGA with genetic algorithms was used in forward modelling and inversion.		
9) DATE  28. June 2002	AUTHORIZED BY  This page only  Jarl Johnsen	POSITION  Director of Research

ISBN 82-464-0642-6

**UNCLASSIFIED**

**SECURITY CLASSIFICATION OF THIS PAGE  
 (when data entered)**



## CONTENTS

	Page
1      INTRODUCTION	7
2      EXPERIMENTAL	7
3      FIRST-ORDER GEOACOUSTIC MODEL	11
4      MATCHED FIELD INVERSION	12
5      SENSITIVITY ANALYSIS OF SIMULATED DATA	13
6      SINGLE-FREQUENCY INVERSION	16
7      BROADBAND INVERSION	20
8      SOURCE LOCALIZATION	22
9      SUMMARY AND RECOMMENDATIONS	30
 APPENDIX	
A      THE TIME SERIES	31
B      THE POWER SPECTRA	35
C      A <i>POSTERIORI</i> /DISTRIBUTIONS FROM BROADBAND INVERSION	38
D      A <i>POSTERIORI</i> /DISTRIBUTIONS FROM SOURCE LOCALIZATION	42
References	47
Distribution list	49



## BROADBAND INVERSION AND SOURCE LOCALIZATION OF VERTICAL ARRAY DATA FROM THE L-ANTENNA EXPERIMENT IN 1999

### 1 INTRODUCTION

A matched field processing experiment using a 1040 m hydrophone array was conducted in the Barents Sea from 2 – 8 August 1999 (1)(2). The measurement area was at Nordkappbanken, outside the Tana fiord and the antenna was deployed in an upright L-shape at approximately 320 m depth. In the first report on inversion of vertical array data from 1999, a single charge detonated at range 5.9 km and depth 17 m was studied (3). Inversion was carried out at different frequencies between 22 Hz and 87 Hz using SAGA and genetic algorithms. The OASES module OAST was used as forward model, and the covariance matrix was input to the Bartlett objective function. The geoacoustic model consisted of six layers: semi-infinite vacuum, three water layers, one sediment layer and a semi-infinite substrate layer. Inverting the four parameters water depth, sediment thickness, sediment velocity, substrate velocity, the Bartlett power was computed to be  $-1.4$  dB at 48.9 Hz. Source localization was carried out at different frequencies and usually the range estimate was in the closest cell to the true range using the baseline model with GA estimated water depth, sediment thickness and sediment velocity at 48.9 Hz. The source was generally located at correct depth in the water column.

In this report a total of seven shots are inverted. Both single-frequency and broadband inversion are demonstrated, in addition to broadband source localization. SAGA with OAST as forward model is used. Only data from the vertical array are analysed.

### 2 EXPERIMENTAL

The 1999 experiment using a 1040 m hydrophone array was conducted outside the Tana fiord. The receiver station was onboard R/V H U Sverdrup II, which also deployed and retrieved the antenna. The source vessel K/V Polarvakt sailed three runs deploying explosive charges. Detonation times and source signals (bubble pulse periods) were recorded onboard the source vessel using a single, towed hydrophone. A few days after the acoustic experiment seismic reflection and refraction measurements were carried out from R/V H U Sverdrup II along the three run lines.

The vertical part of the antenna consisted of 21 hydrophones with spacing 10 m. The horizontal part consisted of 10 hydrophones with spacing from 20 m – 240 m as shown in Figure 2.1. The hydrophones had either 12 dB or 32 dB gain. The sampling frequency was 3051.8 Hz, and the data was recorded in sequences of 506 samples with time tagging (GPS time). Hence each sequence lasted 0.1658 s. Detailed descriptions of the array configuration and acquisition system are found in (4) and (5). The tilt of the vertical antenna was monitored continuously during the experiment using three Aquadopp current meters. The current meters were fastened

to the array cable with strips and tapes approximately 194 m, 104 m and 14 m above the lowest hydrophone.

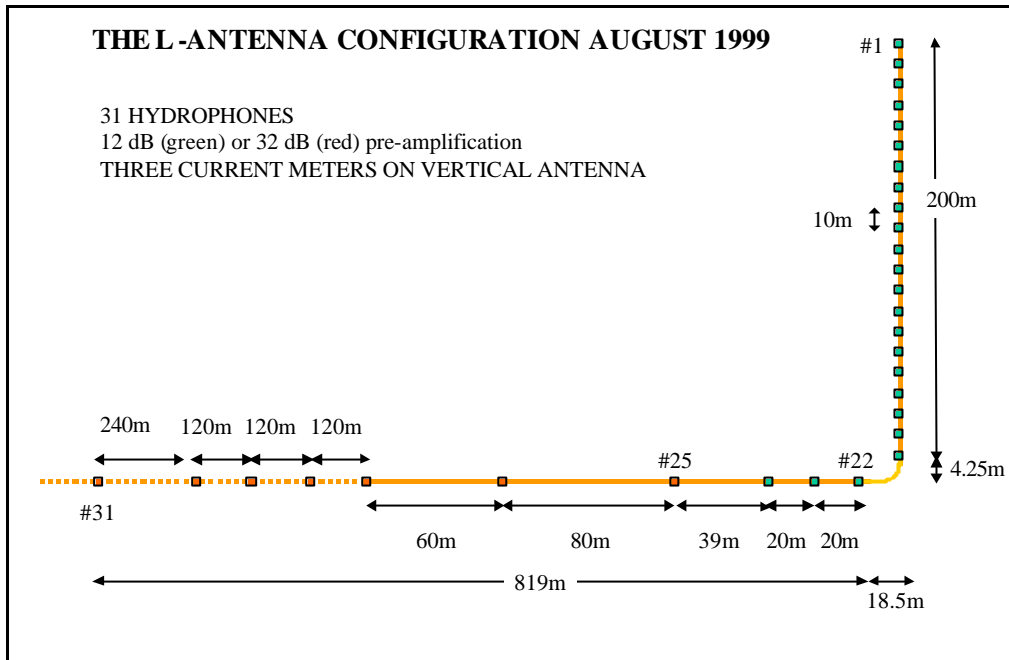


*Figure 2.1 The array configuration in August 1999. The vertical part was ESE of the planned array position. The bearing of the horizontal part was 295.7°.*

In the first run in 1999 the source vessel sailed end-fire towards the antenna. In total seven shots from the last part of run 1 in 1999 are studied in this report. The first shot, # 109, was dropped from the source vessel at 02:15 on 5 August 1999. The last shot, # 115, was dropped at 02:33. As discussed in (3) the maximum horizontal displacement of the vertical antenna due to tide was 4 – 5 m at the end of run 1. The nominal detonation depths alternated between 18 m, 91 m and 244 m, while the actual detonation depths were estimated from the first bubble pulse periods. There was some deviation between nominal and actual source depths, especially for the 91 m and 244 m shots. However, above 40 Hz the source levels should be more or less independent of detonation depths, as shown in Figure 2.2. The position of the source vessel was recorded using a p-code GPS, while the position of the antenna was estimated from the nearest shots (6). The horizontal range between the source and the receiver (vertical array) was estimated using the positioning and geometrical information. The source-receiver range for the seven shots decreased from 8.70 km to 3.17 km. The detonation times, source depths and ranges are listed in Table 2.1. The geometry is illustrated in Figure 2.3. During the seven shots the water depth increased from 342 m to 324 m.

At 02:35 on 5 August, only a few minutes after the last shot, a sound speed profile was measured at the source position using an XCTD (no19). There was a warmer surface layer of thickness 20 – 40 m with sound velocity 1481 – 1488 m/s, and a colder bottom layer with sound velocity down to 1463 m/s, see Figure 2.4. The average sound velocity was 1473 m/s. Computation of the sound speed based on time of detonation, time of arrival and geometric information for shot # 113 confirmed the average value.

The time series are plotted in Appendix A. The data were bandpass filtered 20 - 1000 Hz to avoid low-frequency noise. The arrivals show ray pattern, and surface and bottom reflections are easily observed. The arrivals are easiest to be identified for the shallow shots, which had a bubble pulse period of 120 – 130 ms, see Table 2.2. The deepest shots had a bubble pulse period of only 20 ms, and the shock pulse and the different bubble pulses were soon mixed together. Even if it is easy to observe the arrivals for the shallow shots, the apparently direct pulse may not be the true one due to the downward refracting sound speed profile. Detailed analysis and simulation of one of the shallow shots in (3) showed that the direct pulse and the first-bottom reflected pulse did not arrive the vertical array. The first pulse observed, was the bottom-surface reflected. These effects were not seen for the deeper shots.

The power spectra of the seven shots are plotted in Appendix B. The spectra were computed using a rectangular window and an FFT size of 40 sequences (covering in total 6.6 s and starting about 1 s before the first pulse arrival). The frequency bin was about 0.15 Hz. The bubble pulse periods made the interference pattern in the spectra and the shallow shots exhibited the smallest interference length.

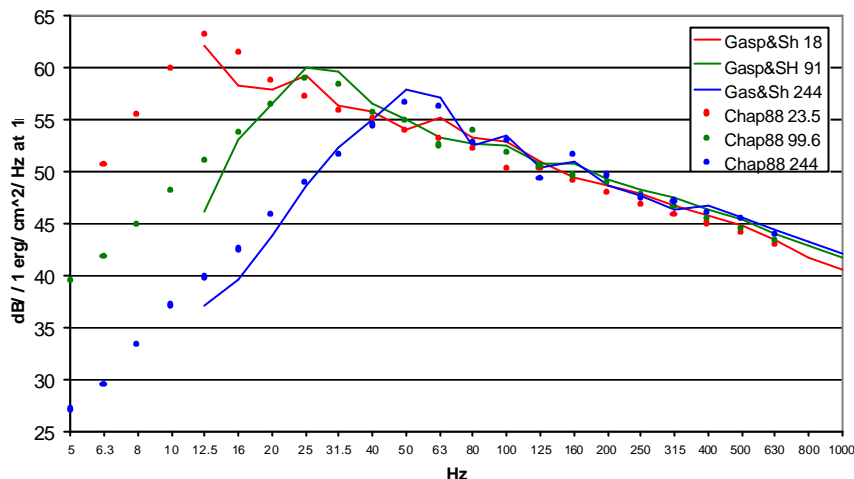


*Figure 2.2 Source levels of 18 m, 91 m and 244 m SUS charges with 0.82 kg TNT (Gaspin and Schuler 1971, N R Chapman 1988).*

Shot number	Source depth (m)	Source-receiver range (km)	Water depth at source position (m)	Drop time (hh:mm)	Recorded time of detonation (hh:mm:ss)
109 S	17.3	8.70	341.8	02:15	02:15:07.6850
110 I	86.2	7.76	337.3	02:18	02:18:17.6480
111 D	241.4	6.83	334.5	02:21	02:21:47.6400
112 S	17.2	5.91	330.8	02:24	02:24:07.5100
113 I	96.1	4.98	327.8	02:27	02:27:19.4390
114 D	247.5	4.07	326.5	02:30	02:30:46.8130
115 S	17.2	3.17	324.0	02:33	02:33:07.5690

*Table 2.1 The source depth and source-receiver range of the shots inverted in the report. All charges had 0.82 kg TNT. The water depths at source positions are also listed. The source depth was estimated from the bubble pulse period measured close to the source position.*

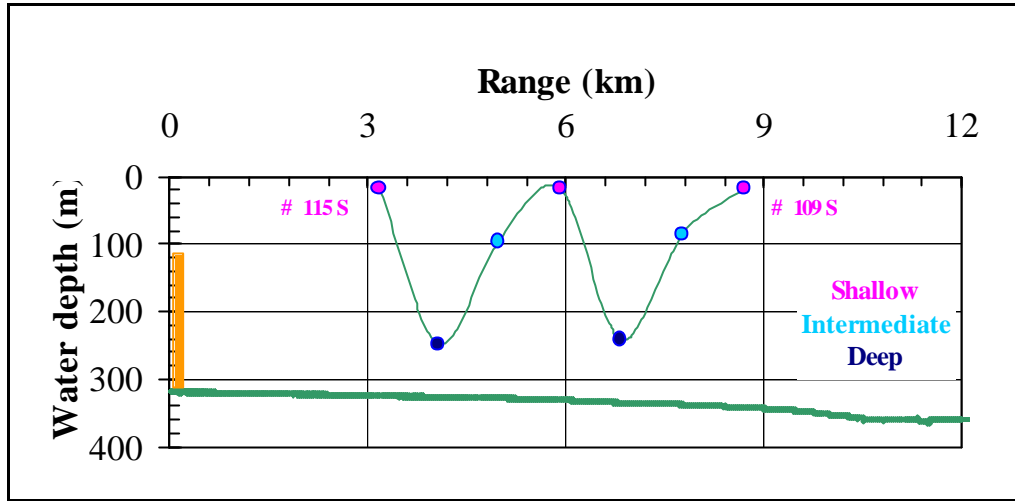


Figure 2.3 The bathymetry measured from the seismic vessel for the last 12 km of run 1. The vertical array is at 0 km. The source-receiver ranges of shots # 109 – # 115 are marked with circles.

Nominal detonation depth	$T_1$	$T_2$	$T_3$
18	123 ms	86 ms	70 ms
91	42 ms	30 ms	24 ms
244	20 ms	14 ms	11 ms

Table 2.2 Theoretical bubble pulse periods of 0.82 kg TNT SUS charges for different source depths.  $T_1$  is the time delay between the shock pulse and the first bubble pulse,  $T_2$  is the time delay between the first bubble pulse and the second bubble pulse etc.

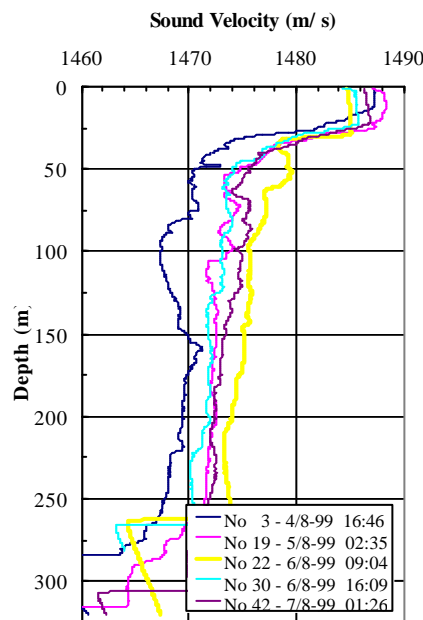


Figure 2.4 Sound velocity profiles measured at the source position (X CTD's).

### 3 FIRST-ORDER GEOACOUSTIC MODEL

The seismic reflection and refraction data was analysed and reported in (7). Analysis of run 1 indicated a two-layer bottom, with a sediment layer above the semi-infinite bedrock. The last 37 km are plotted in Figure 3.1. The sediment layer was assumed having constant sound velocity and density, and no shear. The sediment sound velocity was found to be 1770 m/s. The density in the sediment was estimated from the sound velocity to be 2.0 g/cm<sup>3</sup>. The reflection measurements gave the two-way travel time of the sediment layer. Along run 1 the sediment thickness varied from less than 9 m (the resolution of the system) to 39 m, assuming a sediment sound velocity of 1800 m/s. At the end of run 1, close to the vertical array, the measured two-way travel time was 41 ms indicating a sediment thickness of approximately 37 m (assuming a sound velocity of 1800 m/s).

The bedrock consisted of clay and silt from the Early Cretaceous (~140-100 million years ago). One refraction measurement close to the end of run 1 indicated a sound velocity in the bedrock of 2370 m/s. The shear velocity in the bedrock was estimated from the sound velocity to be 0.9 – 1.1 km/s. The density in the sediment was estimated from the sound velocity to be 2.2 g/cm<sup>3</sup>.

Figure 3.2 shows the first-order geoacoustic (baseline) model for run 1 based on the results from the analysis of the seismic measurements. For simplicity there range- independence and no shear were assumed. The water column was divided into three layers in accordance with the measured sound speed profile. The warmer surface layer was chosen 30 m thick, while the colder bottom layer was chosen to be 44 m thick. The sediment thickness was set to 37 m, and the water depth was set to 319 m. The sediment and substrate velocities were rounded up to 1800 m/s and 2400 m/s, respectively. The sediment attenuations were 0.5 dB/λ and 0.1 dB/λ, respectively.

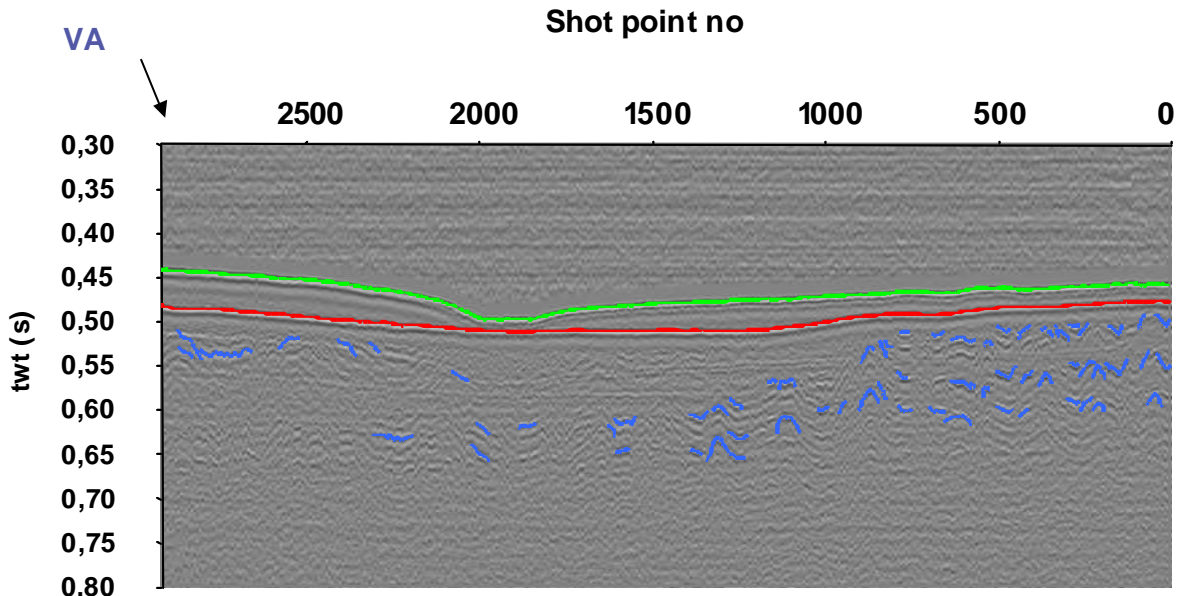


*Figure 3.1 Seismic profile of the last 37 km of run 1 1999. The top sediment is plotted green, while the top bedrock is plotted red. The blue lines indicate minor faults.*

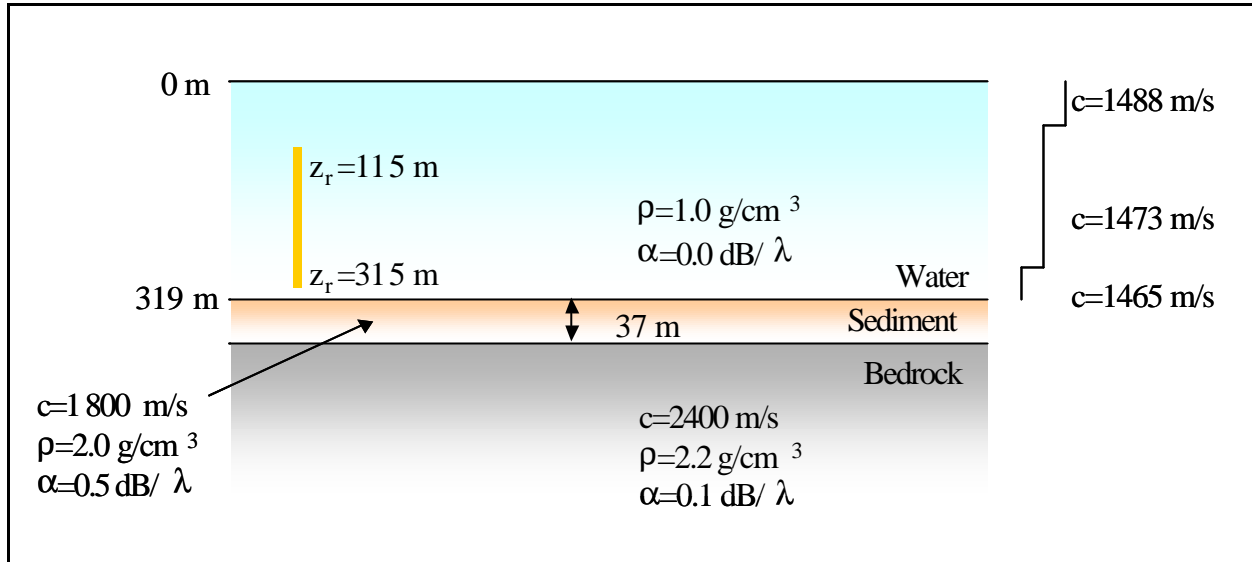


Figure 3.2 The first-order geo-acoustic model used in this report. The water column was divided into three iso-velocity layers.

#### 4 MATCHED FIELD INVERSION

Matched field inversion for geometric and geoacoustic properties was carried out using SAGA (Seismo Acoustic inversion using Genetic Algorithms) (8) (9). The OASES module OAST was used to compute the simulated complex pressure vector (10). The measured covariance matrix R was input to SAGA and the normalized Bartlett processor  $\Phi$  was selected for the objective function:

$$\Phi(\mathbf{m}) = 1 - \frac{1}{N_f} \sum_f \frac{\mathbf{q}^* \mathbf{R} \mathbf{q}}{\|\mathbf{p}\|^2} \quad (4.1)$$

where  $\mathbf{m}$  is the model vector,  $\mathbf{R}$  is equal to the outer product of the measured, complex pressure vector  $\mathbf{p}$  and  $\mathbf{q}(\mathbf{m})$  is the normalized simulated pressure vector from the forward modelling. The summation is over frequency. In order to normalize the covariance matrix,  $\mathbf{R}$  is divided by the norm squared of the pressure vector. With perfect match between the simulated and measured data the value of the objective function (i.e. the energy) is zero, and if no match the energy is 1. Another common measure of the match is the Bartlett power given as

$$BP(\text{dB}) = 10 \log(1 - \Phi) \quad (4.2)$$

Thus the Bartlett power is 0 dB if perfect match and the more negative the value is, the worse the match.

For minimising the objective function, genetic algorithms were used. During optimisation in SAGA version 3.0, the last samples of the search space in each population were stored and used to estimate the *a posteriori* probability distribution of each parameter (8). In version 4.1

all used models in the search were stored and used to compute the *a posteriori* distributions (9).

Based on the *a posteriori* distribution, three estimates of each parameter were available from the post-processor package POST:

- the best of all estimate, associated with the best fit or lowest energy of the objective function (GA best)
- the most likely estimate, based on the peak of the distribution (GA max)
- the mean estimate and standard deviation of the distribution (GA mean)

In addition to plotting the *a posteriori* distributions, the simulated data were compared with measured data across the array (for each hydrophone).

## 5 SENSITIVITY ANALYSIS OF SIMULATED DATA

Sensitivity analysis was carried out in order to determine which parameters were the most sensitive at selected frequencies, hence which parameters would be meaningful to invert. Simulated data was generated and used as input to SAGA. The energy of the Bartlett processor was computed changing only one parameter at a time, while the remaining parameters were kept at their true values (as in the baseline model). Since simulated data was used as input, the energy would be zero when the selected parameter was equal to the true value.

At first, the sensitivity of the parameters characterizing the water layers was studied at 50 Hz, i.e. the sound speed in the upper, middle and lower water layer and depth of upper and middle layer. The source-receiver range was 5.91 km (as for shot #112), while the source depths were 18 m, 91 m or 244 m. Figure 5.1 shows the sensitivity plots for the shallow and deep sources. All five parameters exhibited low sensitivity to deviation from their true values for the shallow source. The most sensitive parameter was the sound speed in the middle layer. For sources at both 91 m and 244 m, all parameters became more sensitive, however not dramatically, and the energy never became 1 (no match) within the search spaces selected.

Secondly, the sensitivity of the parameters characterizing the sediment and substrate were studied at 50 Hz and 128 Hz for an 18 m shot at range 5.91 km, i.e. the water depth, sediment thickness, sediment velocity, sediment attenuation, sediment density and substrate velocity. In addition, the sensitivities of the source depth and source-receiver range were checked to study the effect of any measurement uncertainties. The source depth varied  $\pm 10$  m from the baseline value, while the range varied  $\pm 400$  m. The two most sensitive parameters were the water depth and the source-receiver range, as shown in Figure 5.2. The energy increased dramatically outside a small interval around the true values. The source depth was most sensitive at the highest frequency. There was some sensitivity for the sediment thickness at 50 Hz, but almost no sensitivity at 128 Hz. The sediment velocity was sensitive at both frequencies. The attenuation and density in the two bottom layers were not at all sensitive. Also the sensitivity of the substrate velocity was low. Changing the source depth from 18 m to 244 m, did not change the sensitivities essentially.

To conclude, the sensitivity analysis indicated that for frequencies between 50 Hz and 128 Hz, the main parameters to invert were the water depth, sediment velocity and maybe the sediment thickness. Only large deviations in the parameters characterizing the water column would be influencing the match.

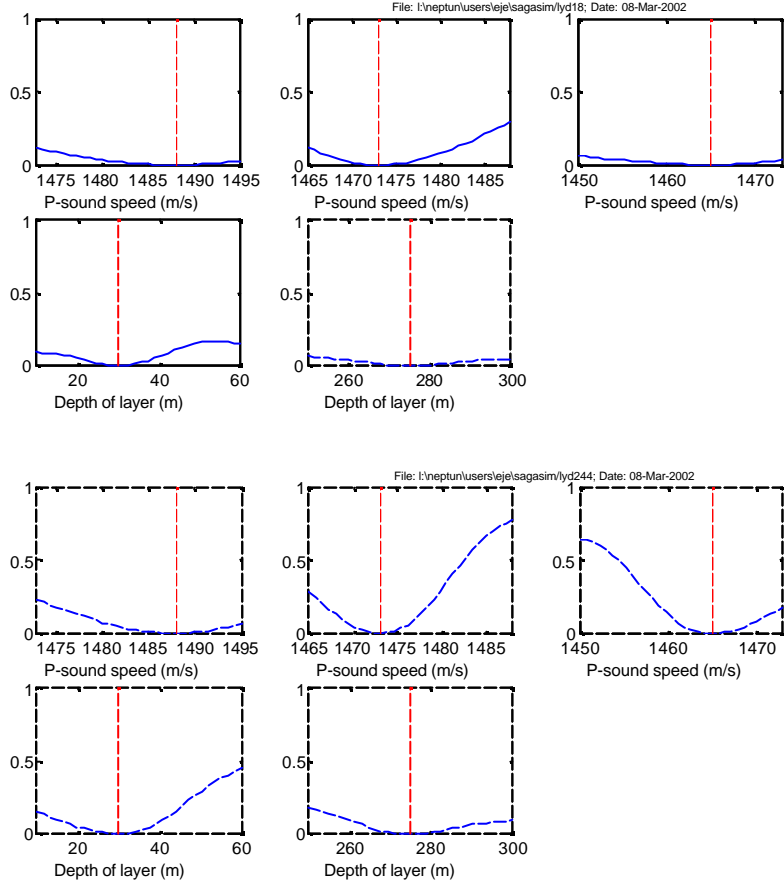


*Figure 5.1 Sensitivity analysis of simulated data at 50 Hz for source depth 18 m (upper) and 244 m (lower). Simulated input data. Baseline model. Source-receiver range 5.91 km. The parameters checked were from left to right and top to bottom: sound speed in the upper, middle and lower water layer, depth of the upper water layer and depth of the middle water layer.*

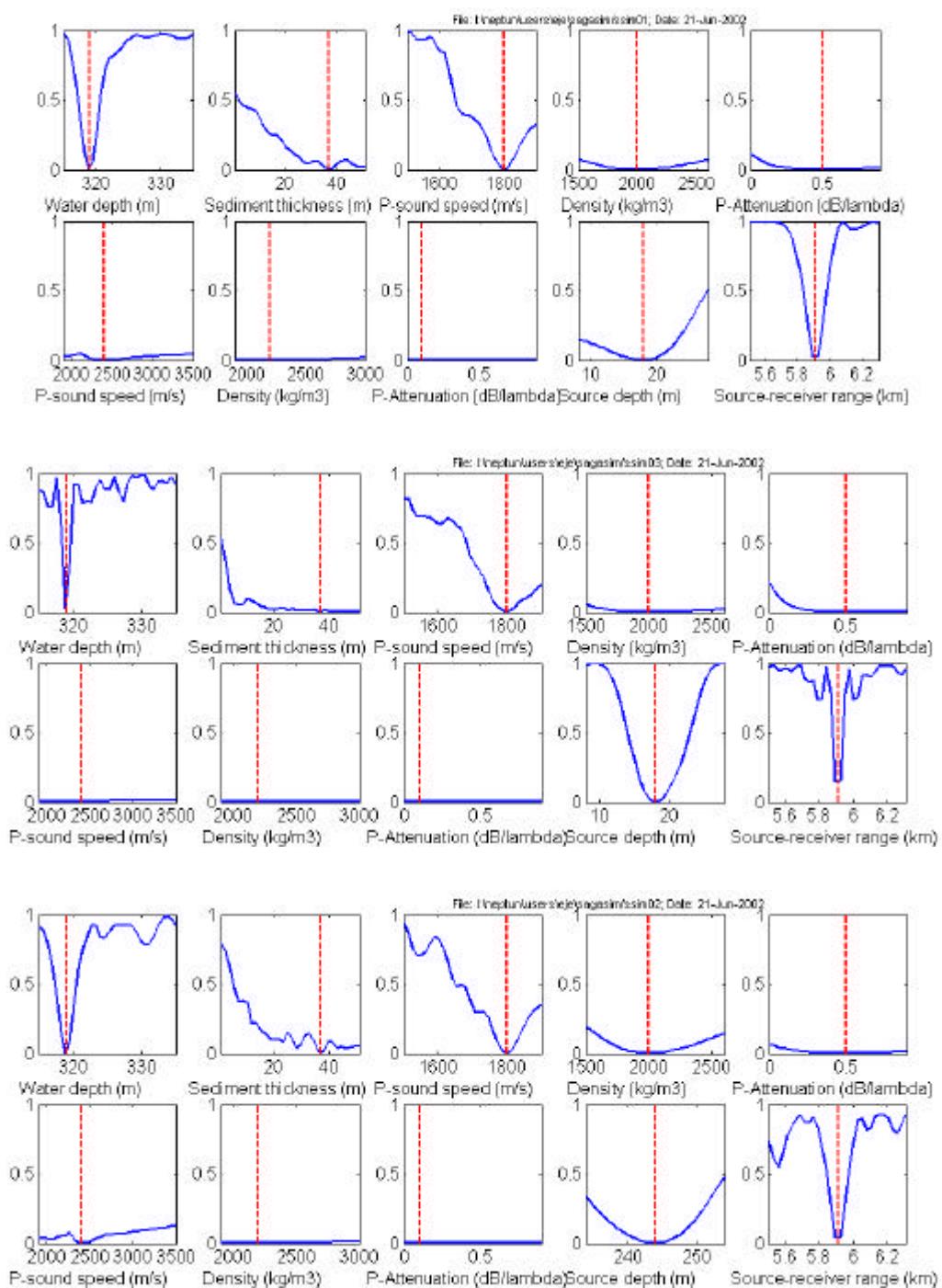


*Figure 5.2 Sensitivity analysis of simulated data. The energy of the Bartlett processor is plotted for selected parameters. Baseline model. Source-receiver range 5.91 km. Upper: 50 Hz, source depth 18 m. Middle: 128 Hz, source depth 18 m. Lower: 50 Hz, source depth 244 m. The parameters were from left to right and top to bottom: water depth (depth of layer), sediment thickness (layer thickness), sound speed in sediment, sediment density, sediment attenuation, sound speed in substrate, substrate density, substrate attenuation, source depth and source-receiver range.*

## 6 SINGLE-FREQUENCY INVERSION

At first, inversion was carried out at single frequencies. The pre-processing of the measured data was carried out using the interactive data language IDL for Windows. At first, the frequency spectrum of each shot was computed based on 40 data sequences covering in total 6.6 s of the time signal, starting about 1 s before the first pulse arrival. Next, the measured covariance matrix was computed at selected frequencies. The covariance matrix was input to SAGA version 3.0, and inversion was carried out separately at each of selected frequencies. The four parameters inverted were: water depth, sediment thickness, sediment velocity and substrate velocity. Even if the sensitivity analysis indicated that the substrate velocity was not sensitive at 50 Hz and 128 Hz, it was chosen to invert this parameter also.

In total 40 inversions between 35 - 206 Hz were carried out, see Table 6.1. Usually frequencies with high signal-to-noise ratios (10 - 30 dB) were selected, and occasionally frequencies with lower signal-to-noise ratios. The parameter search spaces were made wide to be certain to cover the best model (or best model vector) and to check if non-physical models popped up, which could indicate discrepancies in the baseline model or that range independence could not be assumed. Each search space was discretized into 128 values and the increments for the water depth, sediment thickness, sediment velocity and substrate velocity were 0.2 m, 0.4 m, 3 m/s and 13 m/s, respectively, see Table 6.2. The number of parallel population was usually 25, 50 or 100 and the number of forward modelling runs for each population was 1000, 2000 or 4000 dependent on the frequency, as higher frequency data required more computer time. Each population contained 64 individuals. The crossover rate, reproduction size and mutation rate were 0.8, 0.5 and 0.05, respectively.

Figure 6.1 shows the Bartlett power for each of the 40 inversions. At the best, the Bartlett power was -0.9 dB, which was obtained for the shallow shot # 115. None of the inversions of the deep shots (shot # 111 and shot # 114) had a Bartlett power better than -3.0 dB. Inversions of the shallow 18 m shots usually resulted in higher matches than inversions of the intermediate and deep sources.

The water depth estimates varied between less than 315 m (i.e. the lower search bound) to more than 335 m (i.e. the upper search bound), see Figure 6.2. The variation was larger for the deep shots than for the shallow shots. Plotting the average water depth between the source and receiver position, a tendency of smaller depths estimates at closer ranges (higher shot numbers) were observed. The sediment velocity estimates varied from less than 1500 m/s (i.e. the lower search bound) to 1880 m/s, see Figure 6.2. However, no correlation of sediment velocity estimate with inversion frequency was found. Of the 40 inversions carried out 21 estimated the sediment velocity to be lower than 1600 m/s. In eight of the inversions the estimate was between 1600 m/s and 1700 m/s. Hence the velocity estimates were considerably lower than in the baseline model. The sediment thickness estimates varied between 1 m and 44 m, see Figure 6.3. For some of the shots there was a tendency towards thicker layer estimates at lower frequencies, as would have been expected since lower frequencies illuminate the bottom better. However for other shots, the variation was unsystematically with frequency. Estimates of the substrate velocity are plotted in Figure 6.3, and varied from 1910 m/s to more than 3500 m/s (i.e. the upper search bound). This large variation was in

accordance with the sensitivity analysis, which indicated that the substrate velocity would be difficult to estimate at frequencies between 50 Hz and 128 Hz. To conclude, the single-frequency inversion estimates varied largely from frequency to frequency and from shot to shot. The best results were obtained for the shallow 18 m shots.

In order to check the inversion results, sensitivity analysis was carried out at a single frequency using the measured data as input. First, the baseline model was used describing the environment. Next, four of the parameters were changed in accordance with the results from the inversions. Figure 6.4 shows the sensitivity at 48.9 Hz of shot # 112 (shallow). With the baseline model, some sensitivity was observed for the water depth, sediment velocity and source-receiver range, but the energy was not better than 0.5. The sensitivity was much lower than in the sensitivity analysis of simulated data discussed in Chapter 5. Changing the water depth, sediment velocity, substrate velocity and sediment thickness to the estimated values from the single-frequency inversion, the sensitivity increased dramatically. A local minimum was observed for the water depth, sediment velocity and source-receiver range. Unfortunately, the results were not as good for the intermediate and deep sources. Figure 6.5 shows the results of a sensitivity study of shot # 111 (deep) at 48.9 Hz. For the baseline model the energy was low over the entire search spaces. For the modified baseline model (taken into account the results from the inversion), the sensitivity improved some, however not as much as for the shallow shot.

<b>Frequency #</b>	<b># 109 S</b>	<b># 110 I</b>	<b># 111 D</b>	<b># 112 S</b>	<b># 113 I</b>	<b># 114 D</b>	<b># 115 S</b>
1	40.4	48.9	35.3	19.9	47.5	35.3	40.4
2	48.9	73.6	48.9	40.4	48.9	48.9	48.9
3	87.6	92.9	92.9	48.9	73.6	92.9	73.6
4	92.9	119.6	131.2	87.6	74.6	134.3	128.0
5	128.0	163.3	156.2	92.9	126.2	156.2	168.9
6	168.9		206.1	128.0	128.0		
7				168.9			

*Table 6.1 In total 40 separate inversions were carried out for the seven shots at frequencies between 35 – 206 Hz.*

<b>Parameter</b>	<b>Lower bound</b>	<b>Upper bound</b>	<b># discrete values</b>	<b>Increment</b>
Water depth	315 m	335 m	128	0.16 m
Sediment thickness	1 m	51 m	128	0.39 m
Sediment velocity	1500 m/s	1900 m/s	128	3.1 m/s
Substrate velocity	1900 m/s	3500 m/s	128	12.6 m/s

*Table 6.2 Four parameters were inverted at single frequencies. The search spaces and increments are listed.*

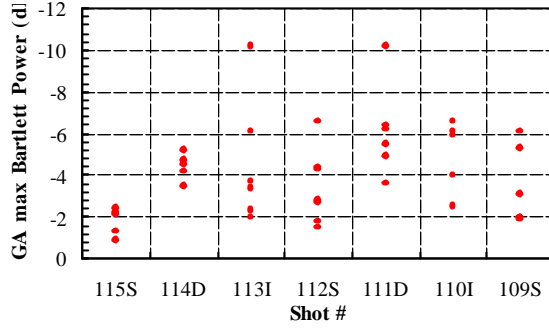


*Figure 6.1 The GA max Bartlett power vs shot number. The Bartlett power varied between  $-0.9$  dB and  $-10.2$  dB. The best matches were obtained for the shallow 18 m shots.*

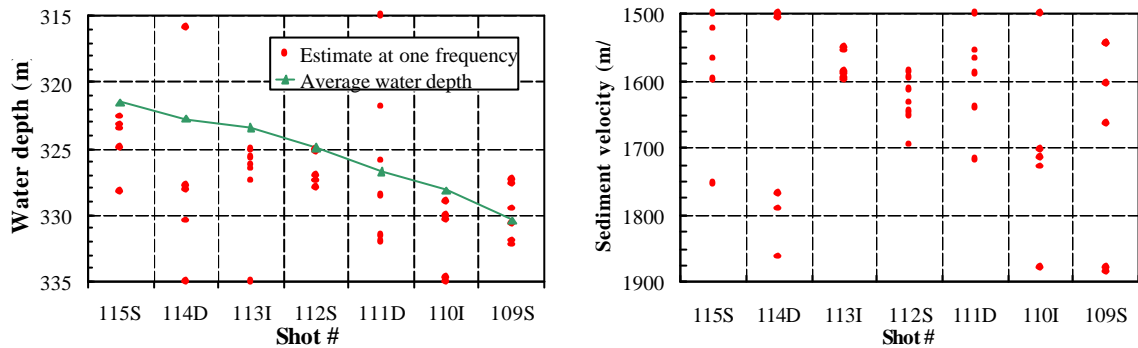


*Figure 6.2 Left: The GA max estimates of water depth vs shot number. The estimates varied from less than 315 m (i.e. the lower search bound) to more than 335 m (i.e. the upper search bound). The average water depth between source and receiver position is plotted for comparison. Right: The GA max estimates of sediment velocity vs shot number. The baseline value was 1800 m/s. More than half of the estimates were below 1700 m/s.*

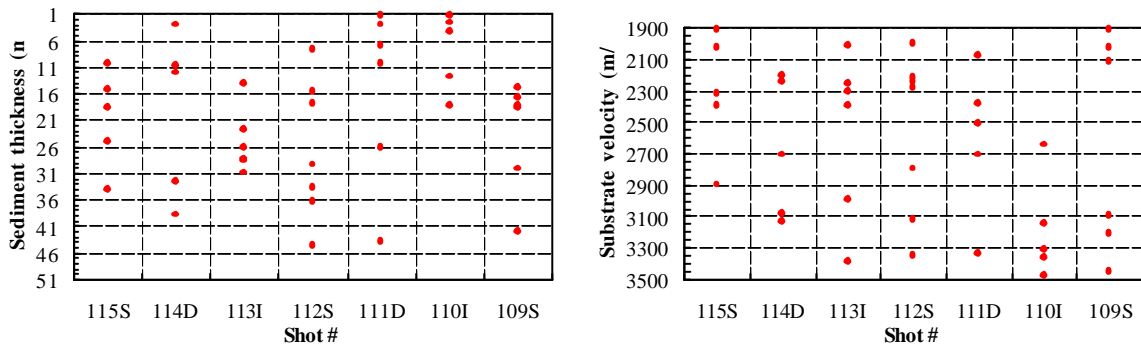


*Figure 6.3 Left: The GA max estimates of sediment thickness vs shot number. The estimates varied between 1 – 44 m, while the baseline value was 37 m. Right: The GA max estimates of substrate velocity vs shot number. The baseline value was 2400 m/s.*

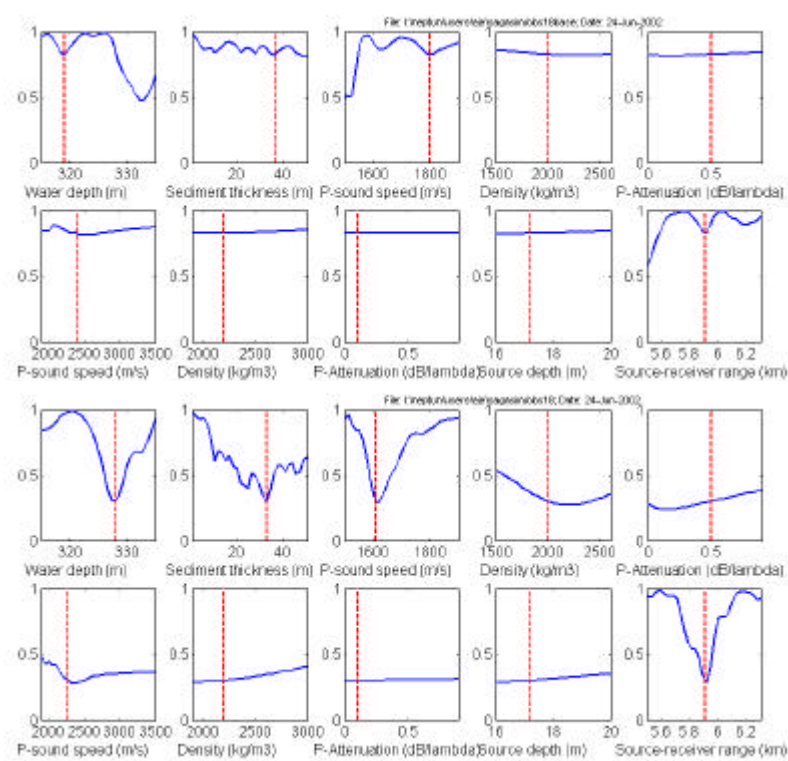


**Figure 6.4** Sensitivity analysis of measured data at 48.9 Hz. Shot #112 S, source depth 17.2 m, source-receiver range 5.91 km. Upper: Baseline model. Lower: Modified baseline model – water depth 328 m, sediment thickness 33.5 m, sediment velocity 1610 m/s and substrate velocity 2280 m/s.

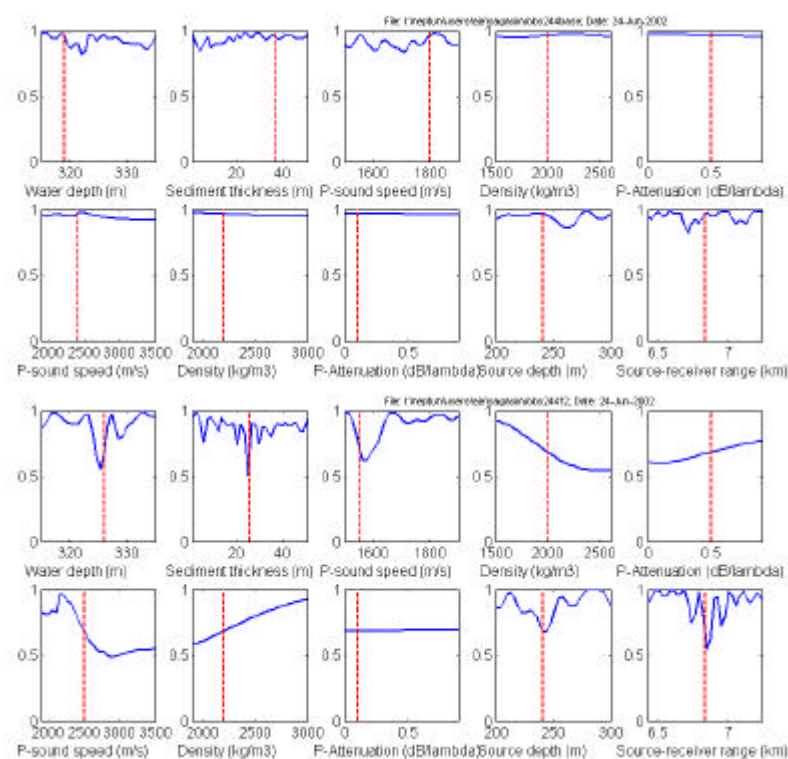


**Figure 6.5** Sensitivity analysis of measured data at 48.9 Hz. Shot #111 D, source depth 241.4 m, source-receiver range 6.83 km. Upper: Baseline model. Lower: Modified baseline model – water depth 326 m, sediment thickness 26 m, sediment velocity 1554 m/s and substrate velocity 2505 m/s.

## 7 BROADBAND INVERSION

Multi-frequency inversion was at first tested for shot # 112 using SAGA version 4.1. Inversion was carried out at 3, 6, 9, 12, 15 and 18 frequencies in order to study the robustness of the parameter estimates as the number of frequencies increased. The frequencies were divided in three bands covering 39.5 - 43.3 Hz, 47.0 - 50.8 Hz and 54.9 - 58.7 Hz, with a step of 0.75 Hz. In total six parameters were inverted: water depth, sediment thickness, sediment velocity, substrate velocity, sediment density and sediment attenuation. As seen in Table 7.1 there was only minor differences in the parameter estimates. It seems like all the estimates stabilize using 12 or more frequencies. With 15 frequencies the water depth was estimated to be 327.6 m, which was 1.2 m deeper than the average value in the single-frequency inversion of shot # 112 (3). The sediment thickness was estimated to be 34.5 m, which was about 8 m thicker than in the single-frequency inversion (3).

Based on the above study, all the seven shots were inverted using 15 frequencies divided in three bands and each band covered 3 Hz, with a frequency step of 0.75 Hz. Since the frequencies were clustered in bands and not separate, the inversion was called broadband instead of multi-frequency. The centre frequencies were

- a) 18 m charges: 41.0 Hz, 48.6 Hz and 56.4 Hz
- b) 91 m charges: 44.3 Hz, 53.7 Hz and 75.1 Hz
- c) 244 m charges: 49.5 Hz, 60.5 Hz and 94.4 Hz

SAGA version 4.1 was used in the inversions. The number of forward modelling runs for each population was 3000. Each population contained 64 individuals and the number of parallel population was reduced to six since all the used models were stored in this version of SAGA. The crossover rate, reproduction size and mutation rate were 0.8, 0.5 and 0.05, respectively. Each search space was discretized into 128 values.

The inversion results of the seven shots are summarized in Table 7.2 (GA best parameter estimates). Some of the results are illustrated graphically in Figure 7.1 and Figure 7.2. The highest Bartlett powers were found for shot # 109, # 112, # 113 and # 115, and three of these were shallow shots. The water depth estimates generally decreased with decreasing range, as expected due to the bathymetry. For all shots, except # 115, the estimates were between the depth at receiver position and depth at source position. From the seismic profiling the sediment thickness was supposed to increase with decreasing range and be less than 37 m at the receiver position, assuming a velocity of 1800 m/s. This tendency was not observed in the broadband inversion. The sediment thickness estimates varied from 34.5 m to 47.5 m, with an average of 40.5 m. The thinnest layers were found for shot # 109, # 112, # 113 and # 115, and three of these were shallow charges. Lower frequencies would penetrate deeper into the bottom, and illuminate the sediment layer better than higher frequencies. With the selected frequency bands for the three source depths, the shallow shots (lowest frequencies) were indeed expected to estimate the thickest layers if constant sediment thickness.

The sediment velocity estimates varied between 1530 m/s and 1650 m/s, which was considerably slower than in the baseline model, and in agreement with the single-frequency

inversion results. However, a sediment thickness of 40.5 m and a velocity of about 1600 m/s were not in accordance with the two-way travel time measured. In order to avoid this conflict and use the *a priori* information in the inversions, the sediment thickness and velocity could have been linked together in the inversion. The GA best substrate velocity estimates varied from 2010 m/s to 3490 m/s, with five of the shots between 2010 m/s to 2220 m/s. The baseline value was 2400 m/s. The baseline density was 2.0 g/cm<sup>3</sup>, and the GA max and BA best density estimates were somewhat higher than this. The baseline sediment attenuation was set to 0.5 dB/λ, while the estimates were considerably lower than this value.

The *a posteriori* probability distributions for all the shots are shown in Appendix C. The water depth, sediment velocity and sediment thickness were well-determined for all seven shots. However, the sediment density and sediment attenuation were not well-determined in any of the shots, and the substrate velocity was well-determined in only some of the shots. These results are in accordance with the sensitivity analysis of simulated data.

Number of frequencies	D (m)	d (m)	c <sub>1</sub> (m/s)	r <sub>1</sub> (g/cm <sup>3</sup> )	a <sub>1</sub> (dB/1)	c <sub>2</sub> (m/s)	Bartlett power (dB)
3	326.6	36.0	1632	1.8	0.11	2253	-2.3
6	327.6	36.4	1626	1.9	0.11	2517	-3.9
9	325.7	25.8	1569	1.9	<0.1	2026	-3.4
12	327.6	34.9	1613	2.1	0.16	2253	-3.1
15	327.6	34.5	1610	2.1	0.16	2215	-2.8
18	327.6	35.3	1613	2.0	0.18	2303	-2.8

Table 7.1 Multi-frequency inversion. GA best parameter estimates for water depth D, sediment thickness d, sediment velocity c<sub>1</sub>, sediment density ρ<sub>s</sub>, sediment attenuation α<sub>1</sub> and substrate velocity c<sub>2</sub>. Shot # 112 S. Source-receiver range 5910 m, detonation depth 17.2 m. SA GA parameters: 3000/64/6.

Shot #	D (m)	d (m)	c <sub>1</sub> (m/s)	r <sub>1</sub> (g/cm <sup>3</sup> )	a <sub>1</sub> (dB/1)	c <sub>2</sub> (m/s)	GA best (dB)	GA start (dB)
109 S	332.2	38.4	1651	<1.8	0.38	3487	-3.3	-12.3
110 I	330.3	42.3	1632	2.3	0.14	2820	-6.9	-13.8
111 D	329.3	46.3	1635	2.4	<0.1	2190	-6.6	-10.5
112 S	327.6	34.5	1610	2.1	0.14	2215	-2.4	-13.7
113 I	327.6	35.6	1623	2.1	0.12	2202	-3.1	-10.3
114 D	322.2	47.5	1528	2.2	0.11	2013	-5.3	-11.7
115 S	327.0	39.2	1639	2.4	0.35	2114	-2.4	-9.8
	<b>319.0</b>	<b>37.0</b>	<b>1800</b>	<b>2.0</b>	<b>0.50</b>	<b>2400</b>	<b>Baseline model</b>	

Table 7.2 GA best parameter estimates for water depth D, sediment thickness d, sediment velocity c<sub>1</sub>, sediment density ρ<sub>s</sub>, sediment attenuation α<sub>1</sub> and substrate velocity c<sub>2</sub>. Baseline model. Multi-frequency (15 frequencies in three bands). SA GA parameters: 3000/64/6.

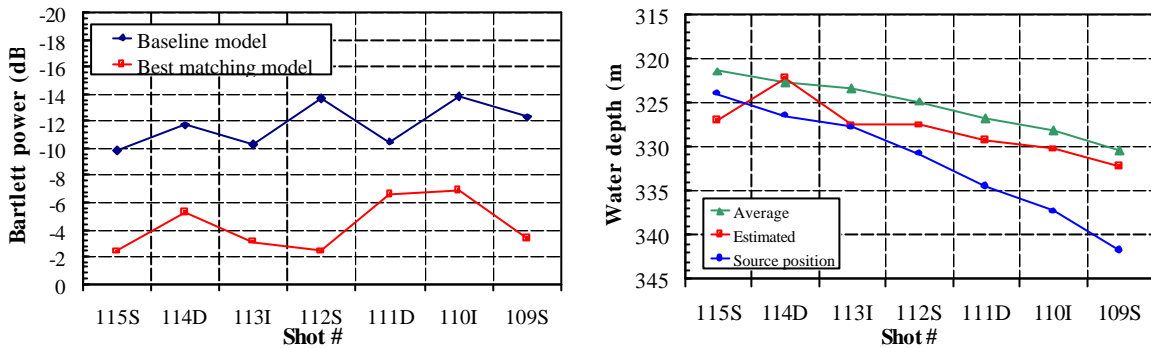


*Figure 7.1 Left: The Bartlett power of the baseline model and the best matching model (lowest energy). Right: The GA best estimates of water depth (pink line) from the broadband inversions.*

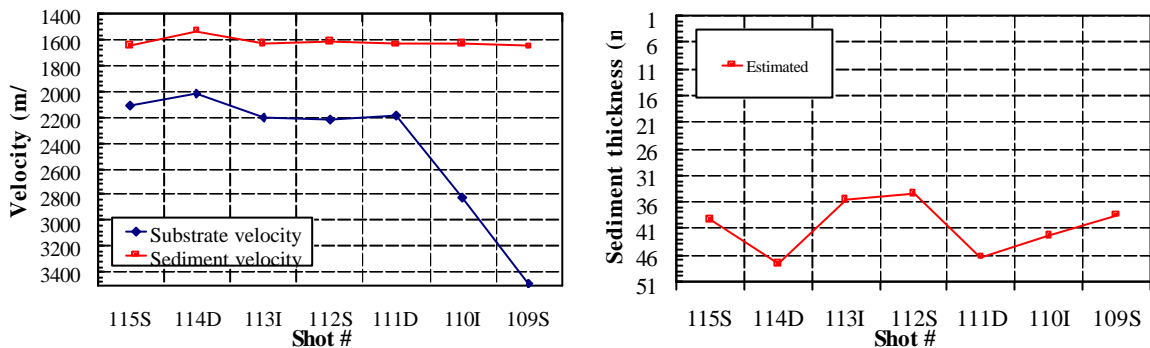


*Figure 7.2 Left: The GA best estimates of sediment velocity and substrate velocity from the broadband inversions. Right: The GA best estimate of sediment thickness from the broadband inversions.*

## 8 SOURCE LOCALIZATION

Broadband localization of the seven sources was carried out using four different environmental models. The geoacoustic parameters were assumed known, and the acoustic field was inverted with respect to source depth and source-receiver range. In total 15 frequencies in three bands were used and the centre frequencies were as in the broadband inversion:

- 18 m charges: 41.0 Hz, 48.6 Hz and 56.4 Hz,
- 91 m charges: 44.3 Hz, 53.7 Hz and 75.1 Hz
- 244 m charges: 49.5 Hz, 60.5 Hz and 94.4 Hz.

The three geoacoustic models were:

BM: Baseline model, inverting source depth and range

M2: Modified model, inverting source depth and range

M3: Modified model, inverting source depth and range, in addition to the water depth

The baseline model was presented in Chapter 3. The modified model differed from the baseline model with a sediment velocity of 1600 m/s instead of 1800 m/s and a sediment

attenuation of  $0.15 \text{ dB}/\lambda$  instead of  $0.5 \text{ dB}/\lambda$ . In model BM and M2 the water depth was fixed to 319 m as in the baseline model. In model M3 the water depth was inverted in order to adjust for the range-dependent bathymetry. The search space for source depth was 5 – 315 m, with resolution 2.5 m. The search space for range was 1 – 30 km, with resolution 100 m. The search space for water depth was 315 – 335 m, with resolution 0.5 m. The number of forward modelling runs was 3000. Each population contained 64 individuals. The localization of the 18 m charges performed well using only one population. For the deeper charges four populations were required to give well-determined estimates. The crossover rate, reproduction size and mutation rate were 0.8, 0.5 and 0.05 respectively. SAGA version 4.1 was used in the localization.

The *a posteriori* distributions are shown in Appendix D and Table 8.1 - Table 8.3 tabulate the GA best estimates of range and source depth for the three models BM, M2 and M3. The GA best range estimates were close to the true ranges for all three models. For model a) the range estimates were only 200 – 1200 m (5 – 15 %) lower than the true values. The GA best depth estimates deviated between 3 – 35 m (9 – 60 %) from the true values. The largest percentage error was found for an 18 m shot, where the estimated depth was 27.5 m and the true depth was 17.2 m. The source depths of the deeper shots were underestimated, while the depths of the 18 m shots were overestimated. Even if the estimates were close to the true values, the *a posteriori* distributions showed several and/or wide peaks, and only looking at the distributions it would be difficult to estimate the range and source depth.

The results improved using model M2. The range errors were only 70 - 500 m (2 – 6 %), while the errors in source depth were between 0.3 – 19 m (2 - 16 %). Still, the *a posteriori* distributions showed multi-peaks. Using the modified baseline model and also inverting the water depth (model M3), the errors in range estimate were about the same, while the errors in depth estimate were between 4 - 16%. The *a posteriori* distributions for range and source depth showed that the parameters were well-determined. Figure 8.1 compares the estimated source positions with the true positions for all seven shots.

Selected ambiguity surface are plotted in Figure 8.2 - Figure 8.5. The resolution in source depth was 10 m, while the resolution in range was 250 m. Generally the number of sidelobes (false sources) was low, probably due to the averaging over 15 frequencies. The clearest peaks were obtained for model M2 or M3. For the intermediate shots, the ambiguity surfaces were difficult to analyse. This could be due to the lower resolution in the ambiguity surfaces compared to the *a posteriori* distributions.

	Range (km)		Source depth (m)		Bartlett power (dB)	
Shot #	True	GA best	True	GA best	GA start	GA best
109 S	8.70	7.9	17.3	20.0	-12.3	-5.1
110 I	7.76	6.6	86.2	55.0	-13.8	-9.6
111 D	6.83	6.3	241.4	220.0	-10.5	-5.9
112 S	5.91	5.4	17.2	27.5	-13.7	-5.3
113 I	4.98	4.6	96.1	87.5	-10.3	-5.0
114 D	4.07	3.8	247.5	212.5	-11.7	-5.8
115 S	3.17	3.0	17.2	22.5	-9.8	-4.9

Table 8.1 The range and source depth estimates for the seven shots using the baseline model – BM. Broadband localization, SA GA parameters: 3000/64/1 (18 m) and 3000/64/4 (91 m & 244 m).

	Range (km)		Source depth (m)		Bartlett power (dB)	
Shot #	True	GA best	True	GA best	GA start	GA best
109 S	8.70	8.2	17.3	20.0	-10.9	-5.5
110 I	7.76	7.3	86.2	82.5	-13.5	-7.7
111 D	6.83	6.5	241.4	222.5	-13.2	-4.8
112 S	5.91	5.6	17.2	20.0	-11.0	-4.5
113 I	4.98	4.8	96.1	87.5	-10.1	-5.5
114 D	4.07	4.0	247.5	232.5	-7.6	-4.9
115 S	3.17	3.0	17.2	17.5	-5.1	-3.9

Table 8.2 The range and source depth estimates for the seven shots using the modified baseline model – M2. Broadband localization, SA GA parameters: 3000/64/1 (18 m) and 3000/64/4 (91 m & 244 m).

	Range (km)		Source depth (m)		Water depth (m)	Bartlett power (dB)	
Shot #	True	GA best	True	GA best	GA best	GA start	GA best
109 S	8.70	8.4	17.3	20.0	325.5	-10.9	-2.9
110 I	7.76	7.3	86.2	82.5	318.5	-13.5	-7.7
111 D	6.83	6.5	241.4	225.0	320.5	-13.2	-4.2
112 S	5.91	5.7	17.2	15.0	323.9	-11.0	-3.2
113 I	4.98	4.8	96.1	90.0	322.5	-10.1	-3.4
114 D	4.07	4.1	247.5	235.0	325.5	-7.6	-3.7
115 S	3.17	3.2	17.2	20.0	325.0	-5.1	-2.6

Table 8.3 The range and source depth estimates for the seven shots using the modified baseline model – M3. The water depth was non-fixed. Broadband localization, SA GA parameters: 3000/64/1 (18 m) and 3000/64/4 (91 m & 244 m).

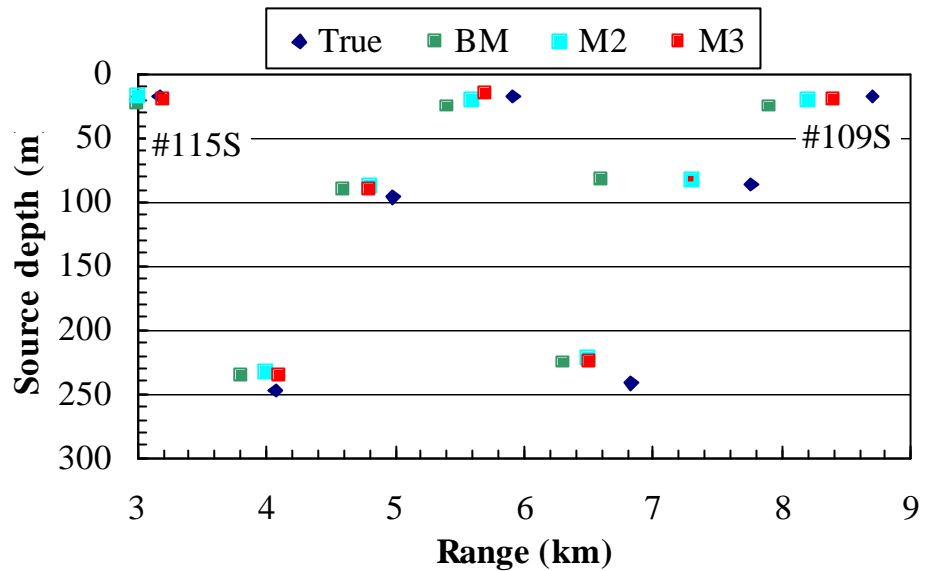
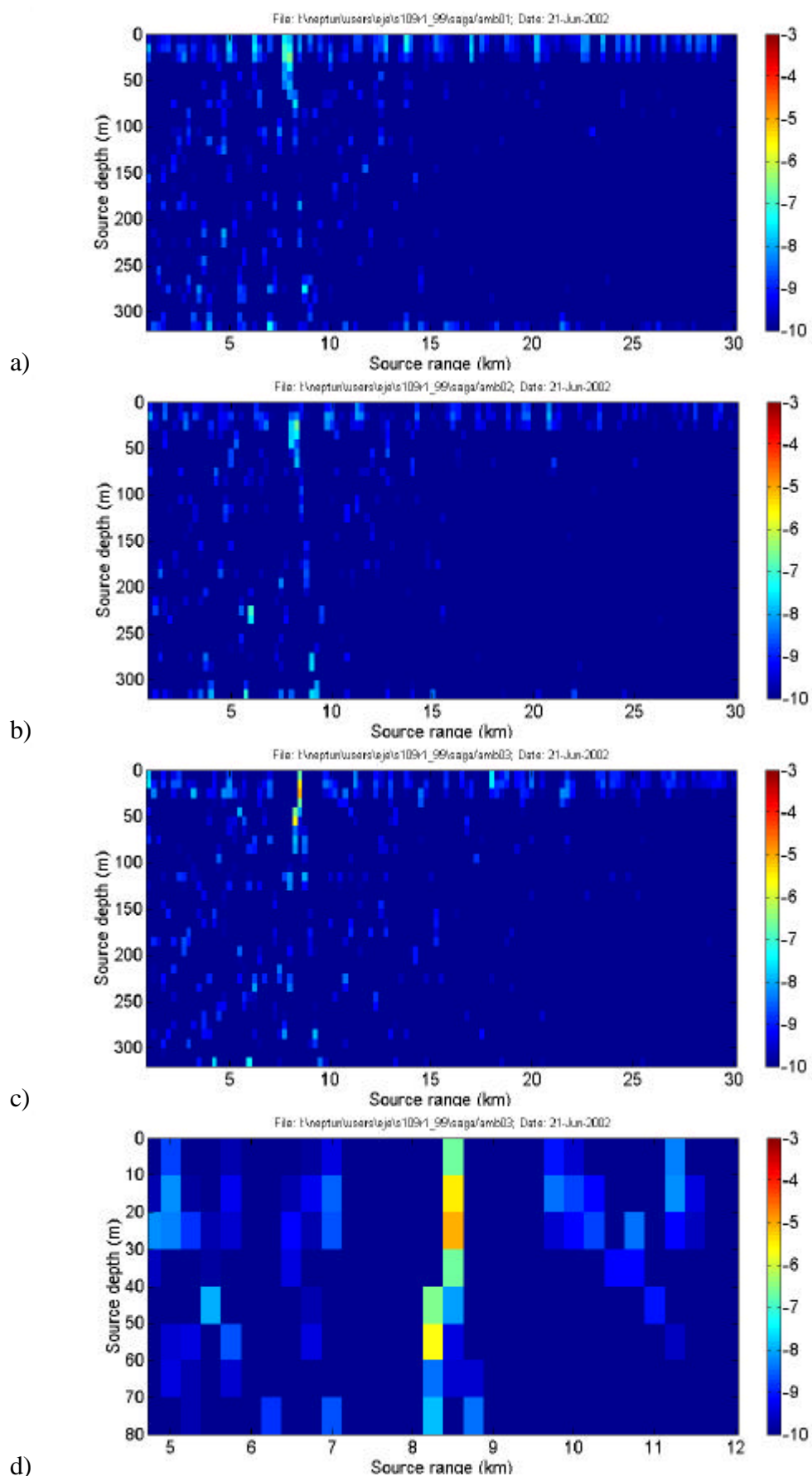
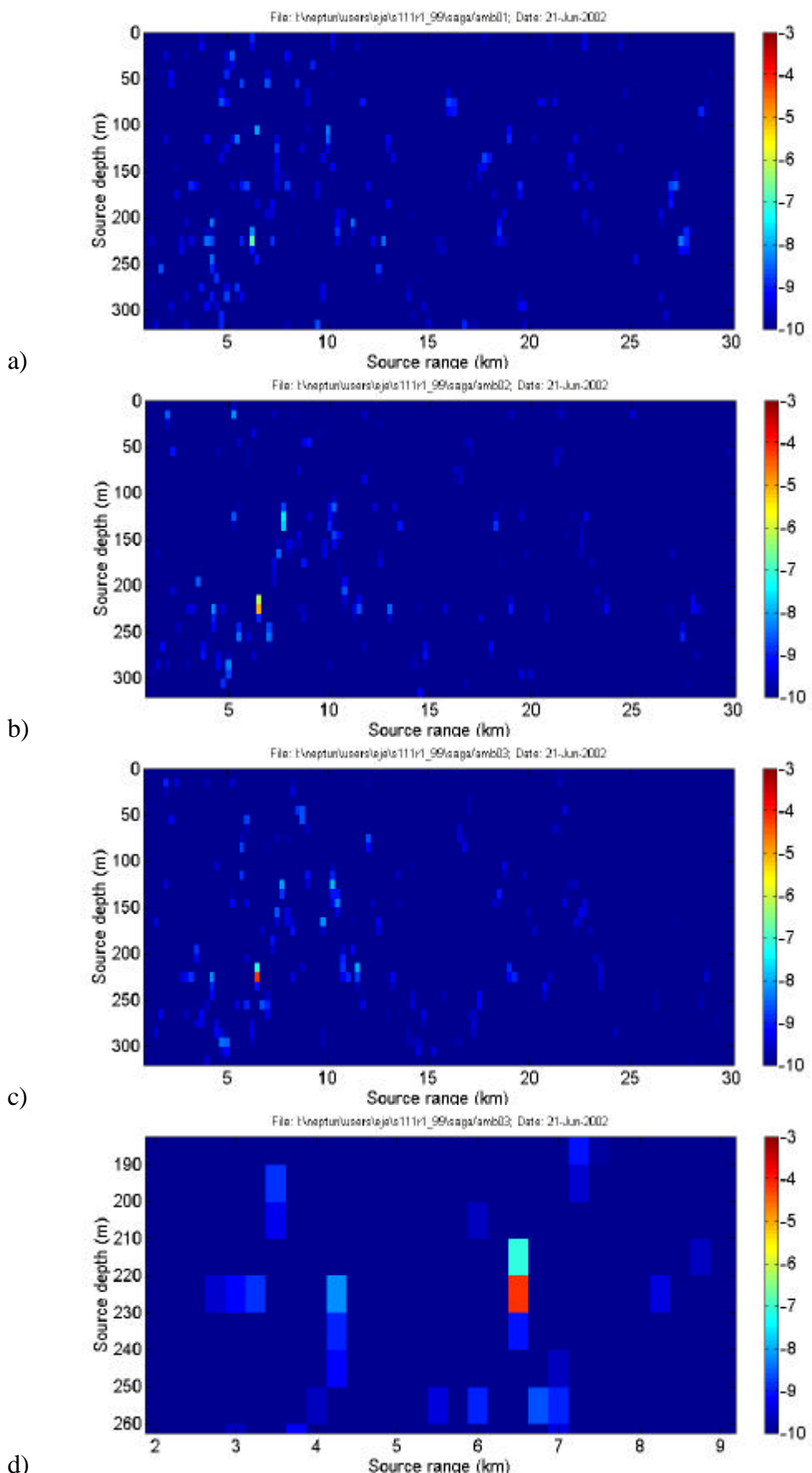


Figure 8.1 The estimated source positions using the baseline model (BM) and model M2 and M3, compared with the true source positions.



*Figure 8.2 The ambiguity surfaces of shot # 109 S. a) Baseline model. b) Modified baseline model. c) Modified baseline model with water depth changed from 319 m to 325.5 m. d) The highest peak was at (8.5 km, 25 m), while the true location was at (8.7 km, 17.3 m).*



*Figure 8.3 The ambiguity surfaces of shot # 111 D. a) Baseline model. b) Modified baseline model. c) Modified baseline model with water depth changed from 319 m to 320.5 m. d) The highest peak was at (6.5 km, 225 m), while the true location was at (6.83 km, 241.4 m).*

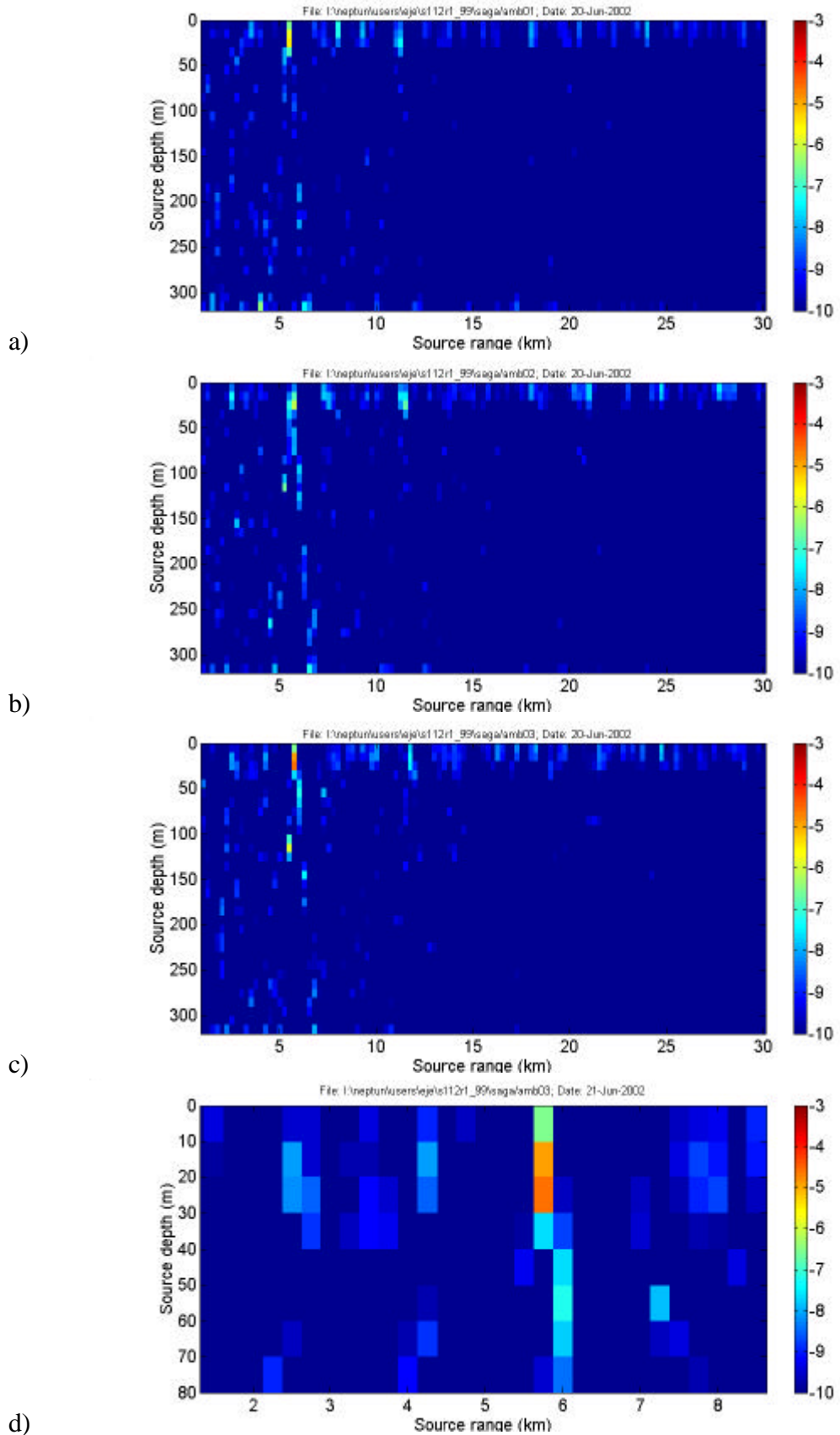


*Figure 8.4 The ambiguity surfaces of shot # 112 S. a) Baseline model. b) Modified baseline model. c) Modified baseline model with water depth changed from 319 m to 323.9 m. d) The highest peak was at (5.75 km, 25 m), while the true location was at (5.91 km, 17.2 m).*

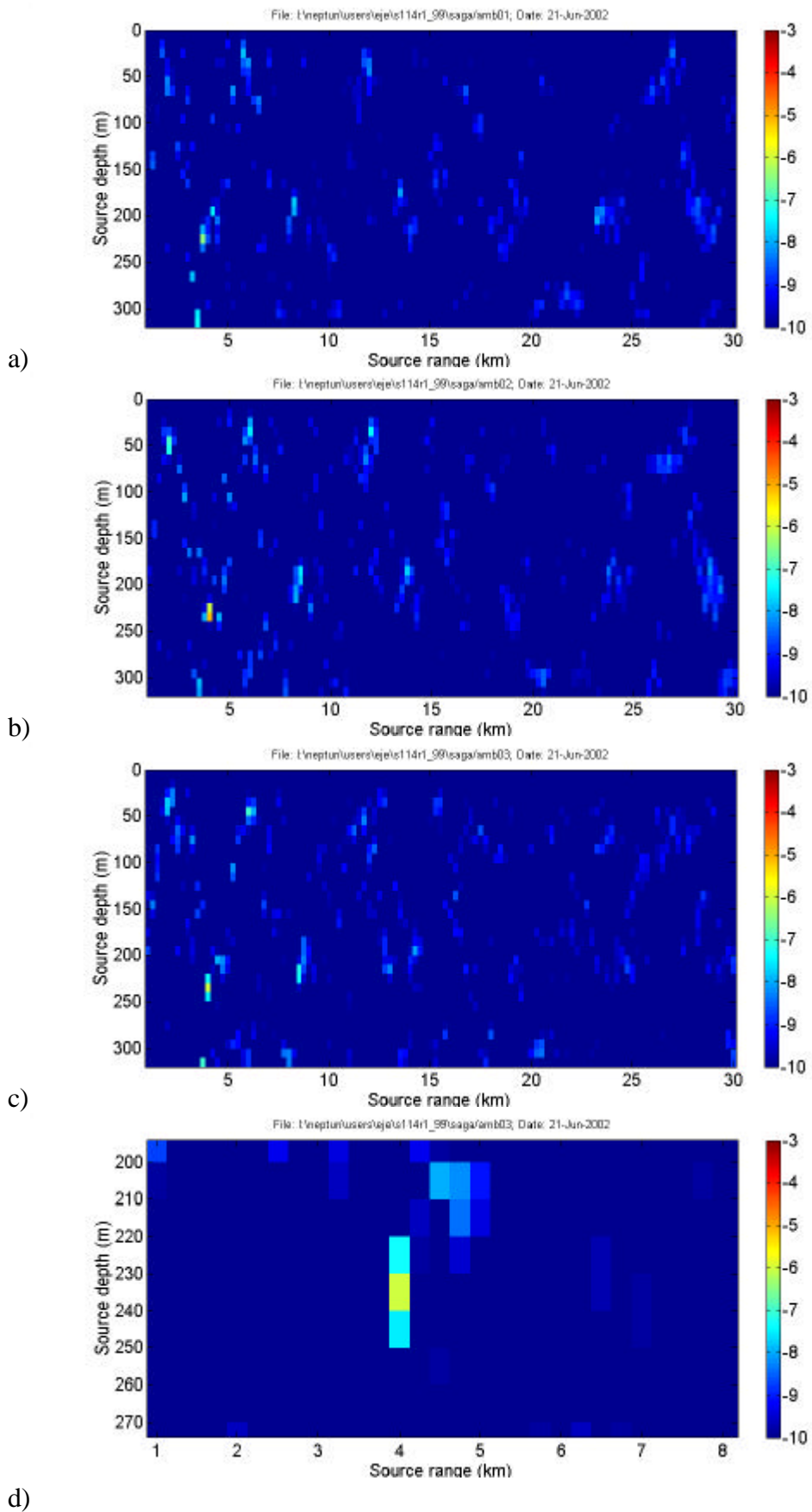


*Figure 8.5 The ambiguity surfaces of shot # 114 D. a) Baseline model. b) Modified baseline model. c) Modified baseline model with water depth changed from 319 m to 325.5 m. d) The highest peak was at (4.0 km, 235 m), while the true location was at (4.07 km, 247.5 m).*

## 9 SUMMARY AND RECOMMENDATIONS

Broadband matched field inversion and processing techniques have been demonstrated in this report using vertical array data. The OASES module OAST and SAGA with genetic algorithms were successfully used in forward modelling and inversion.

The environmental model was assumed range-independent and consisted of three water layers, one sediment layer and a half-space substrate layer. While single-frequency inversions gave varying parameter estimates, broadband inversions proved to be more robust. The sediment velocity estimates were all between 1530 m/s and 1650 m/s and considerably lower than in the baseline model. The sediment thickness was estimated to be in average 40.5 m. The GA best substrate velocity estimates varied from 2010 m/s to 3490 m/s, with five of the shots between 2010 m/s to 2220 m/s. The water depth estimate usually lied between the depth at the receiver position and the depth at the source position, and was to some degree correlated with the bathymetry.

Broadband source localization was studied using three different geoacoustic models. The best matches were found for a modified baseline model when also inverting the water depth. The error in range estimate was only 1 – 6 %, while the error in source depth estimate was 4 – 16 %.

For all three models the source depth was underestimated for the 91 m and 244 m shots, and usually overestimated for the 18 m shots. The range was usually underestimated. The best matches in both inversion and localization were found for the 18 m shots.

For a coming up study the following recommendations are given:

- investigate the theory behind the *a posteriori* distributions and how to improve these
- investigate the lower match in inversion and source localization for medium and deep charges
- validate the results using other forward models

## APPENDIX

### A THE TIME SERIES

Time series from the 21 vertical hydrophones are plotted in Figure A.1 – Figure A.7. The data are from shot # 115 – shot # 109 in run 1, 1999. The source-receiver range was between 8.7 - 3.2 km. The nominal detonation depth alternated between 18 m (shallow), 91 m (intermediate) and 244 m (deep).

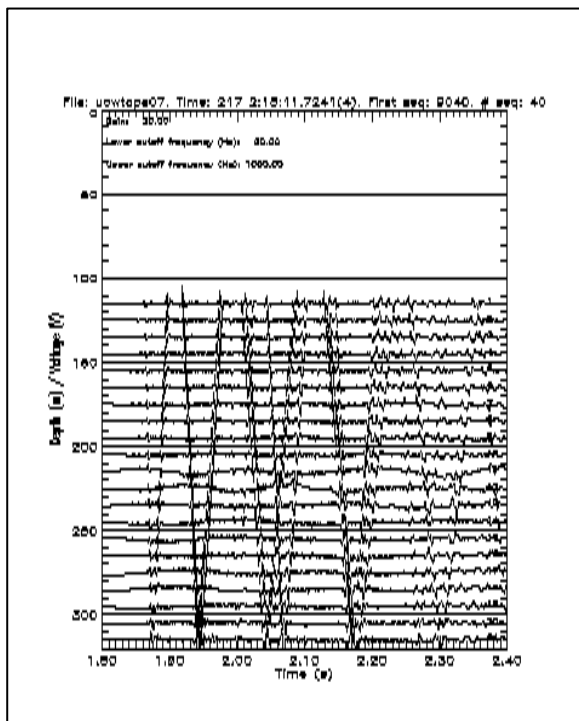


*Figure A.1 The time series of shot # 109 S.*

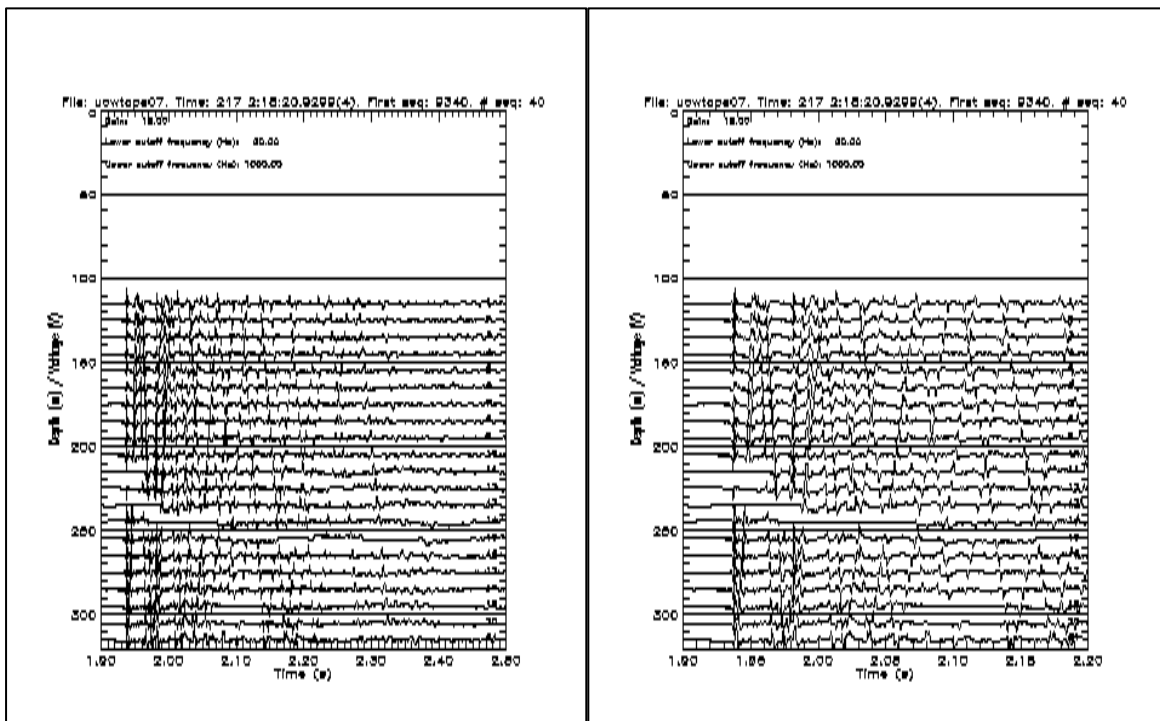


Figure A.2 The time series of shot # 110 I.

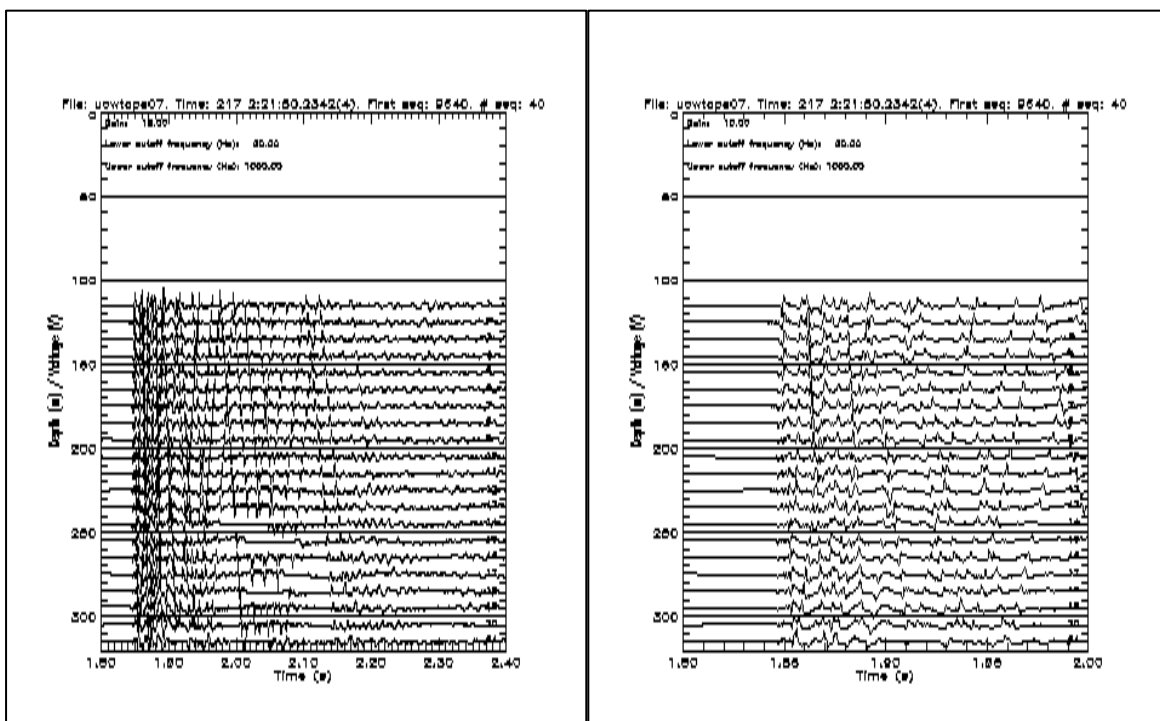


Figure A.3 The time series of shot # 111 D.

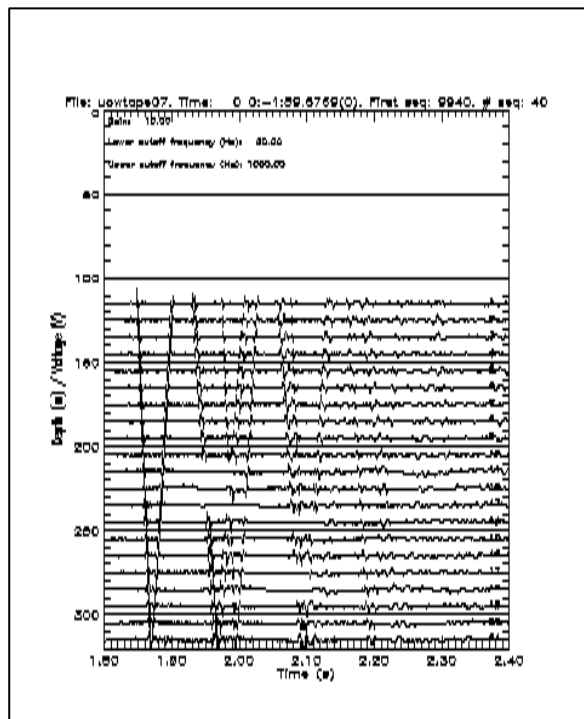


Figure A.4 The time series of shot # 112 S.

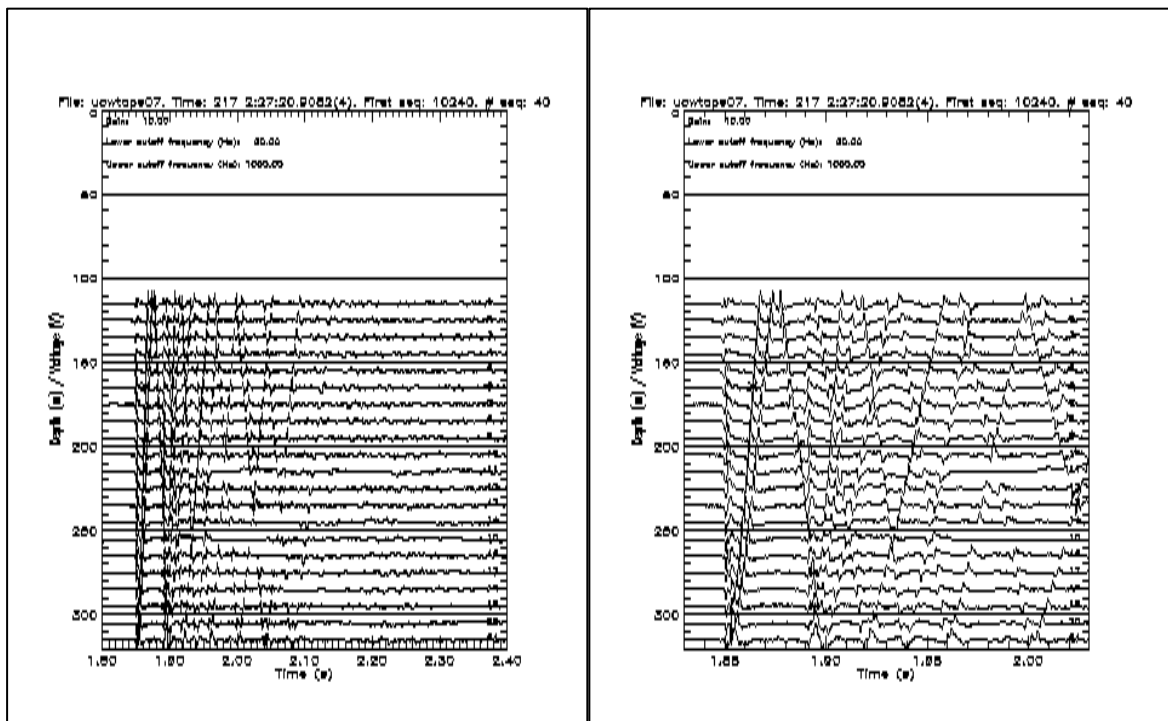


Figure A.5 The time series of shot # 113 I.

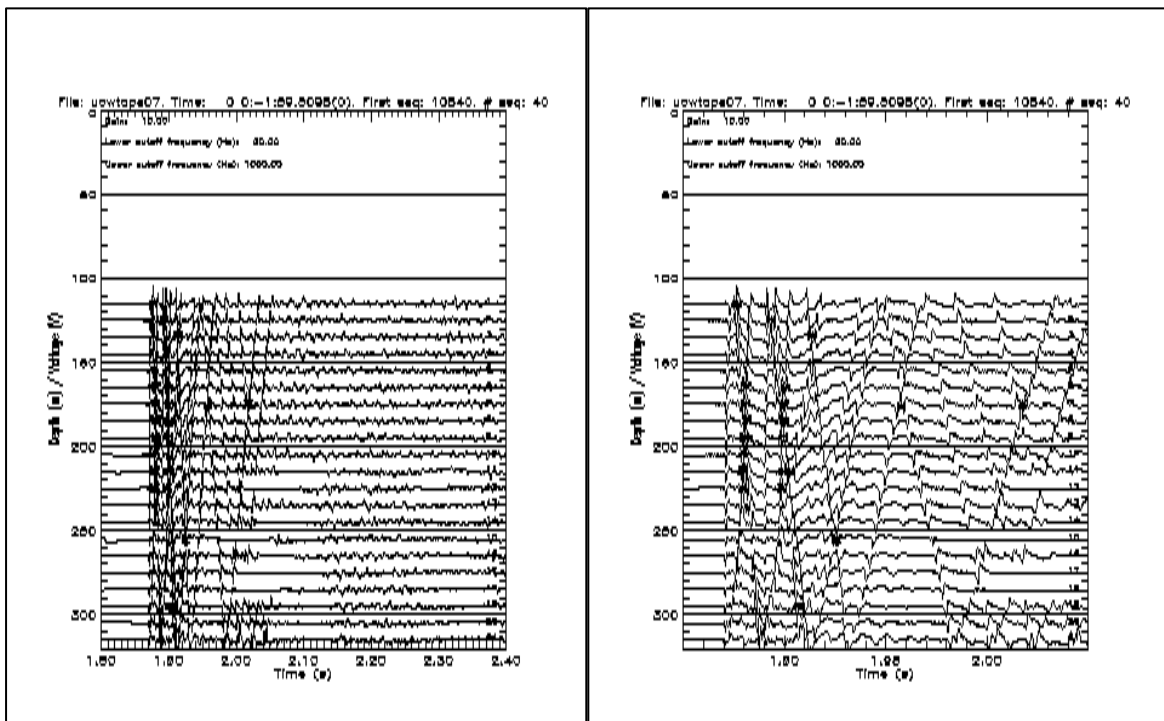


Figure A.6 The time series of shot # 114 D.

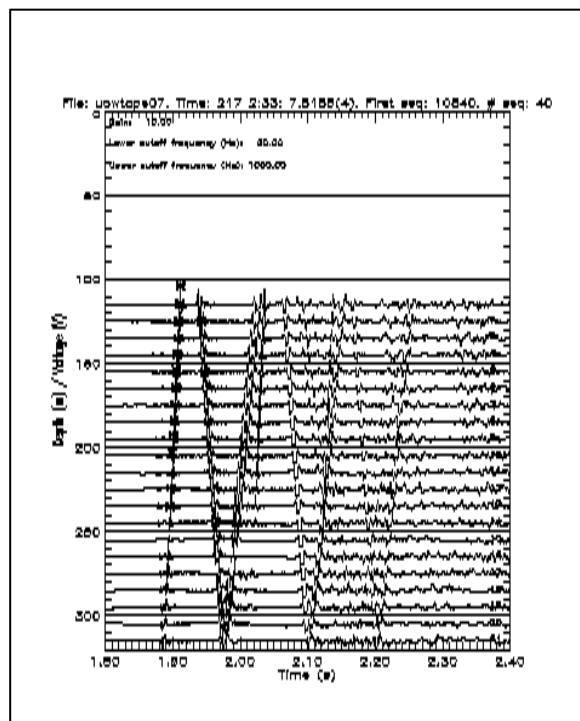
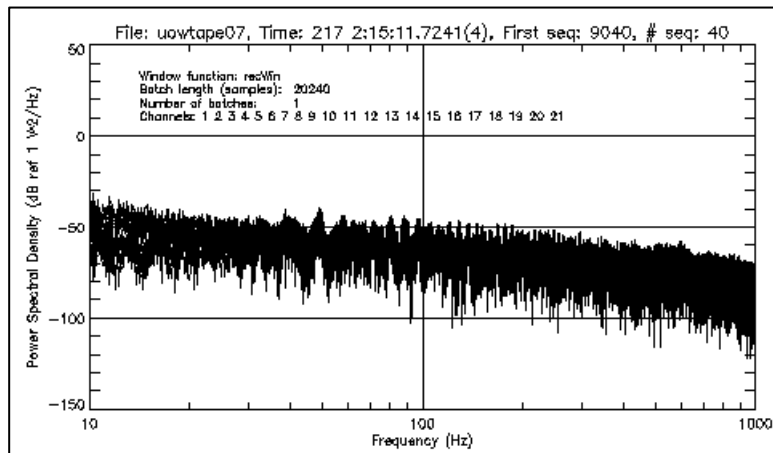


Figure A.7 The time series of shot # 115 S.

## B THE POWER SPECTRA

The power spectra were computed using a rectangular window and an FFT size of 20240 samples (40 sequences) covering 6.6 s of the time series, starting about 1 s before the first pulse arrival. The frequency bin was about 0.15 Hz. The interactive data language IDL for Windows was used for the pre-processing of the data. The covariance matrix was computed at selected frequencies. The nominal detonation depth alternated between 18 m (shallow), 91 m (intermediate) and 244 m (deep). The bubble pulse periods made the interference pattern in the spectra and the shallow shots exhibited the smallest interference length.



*Figure B.1 The power spectral density of shot # 109 S.*

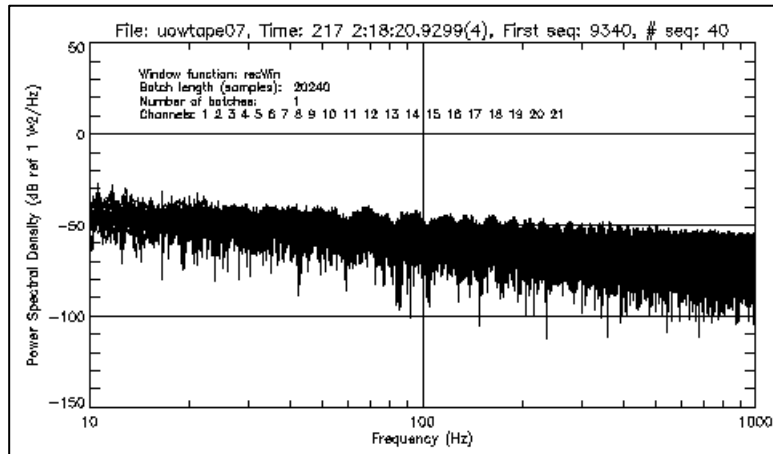


*Figure B.2 The power spectral density of shot # 110 I.*

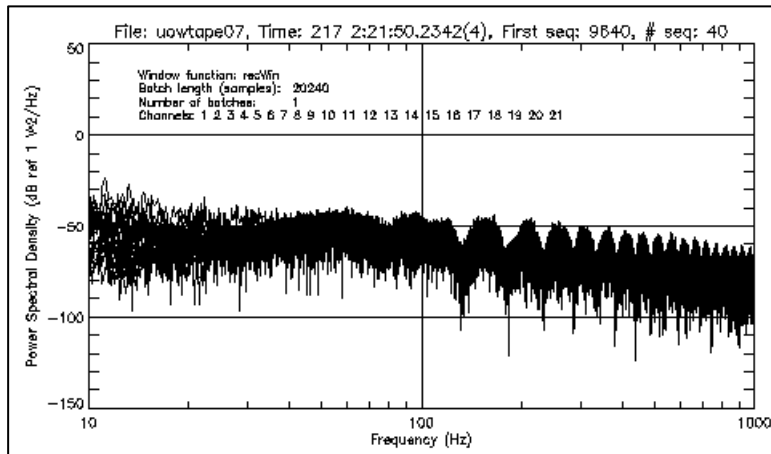


*Figure B.3* The power spectral density of shot # 111 D.

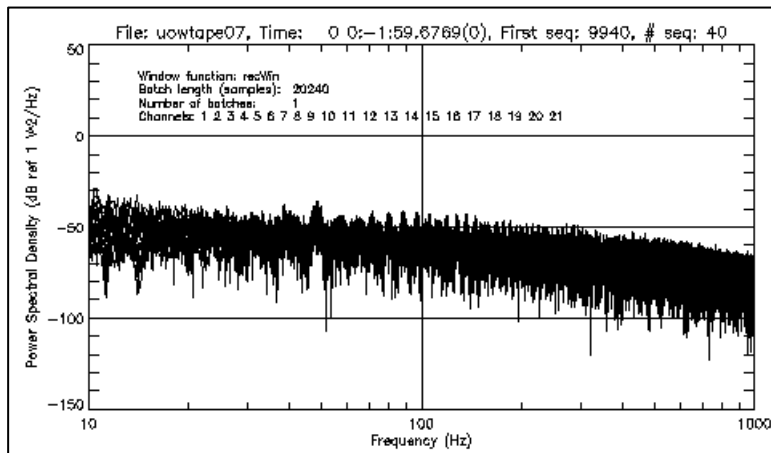


*Figure B.4* The power spectral density of shot # 112 S.

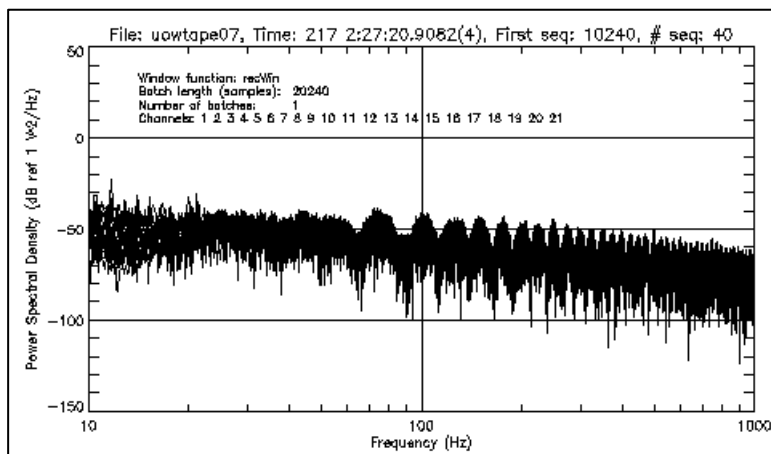


*Figure B.5* The power spectral density of shot # 113 I.

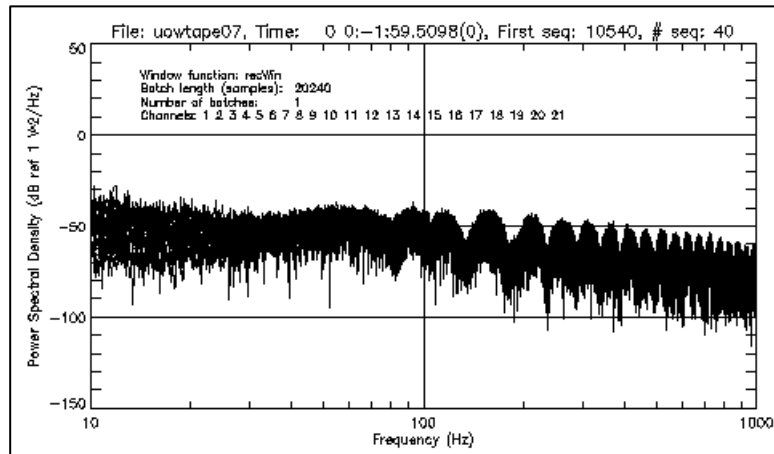


*Figure B.6 The power spectral density of shot # 114 D.*

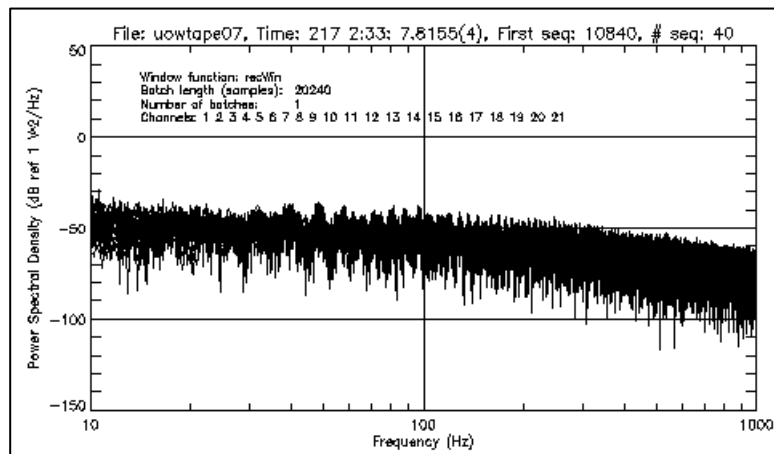


*Figure B.7 The power spectral density of shot # 115 S.*

### C A POSTERIORI DISTRIBUTIONS FROM BROADBAND INVERSION

The *a posteriori* probability distributions from the broadband inversion of the shots # 109 - # 115 are plotted in the below figures. The model that gave the best match is marked as green, dashed lines, while the baseline model is marked as red, solid lines.

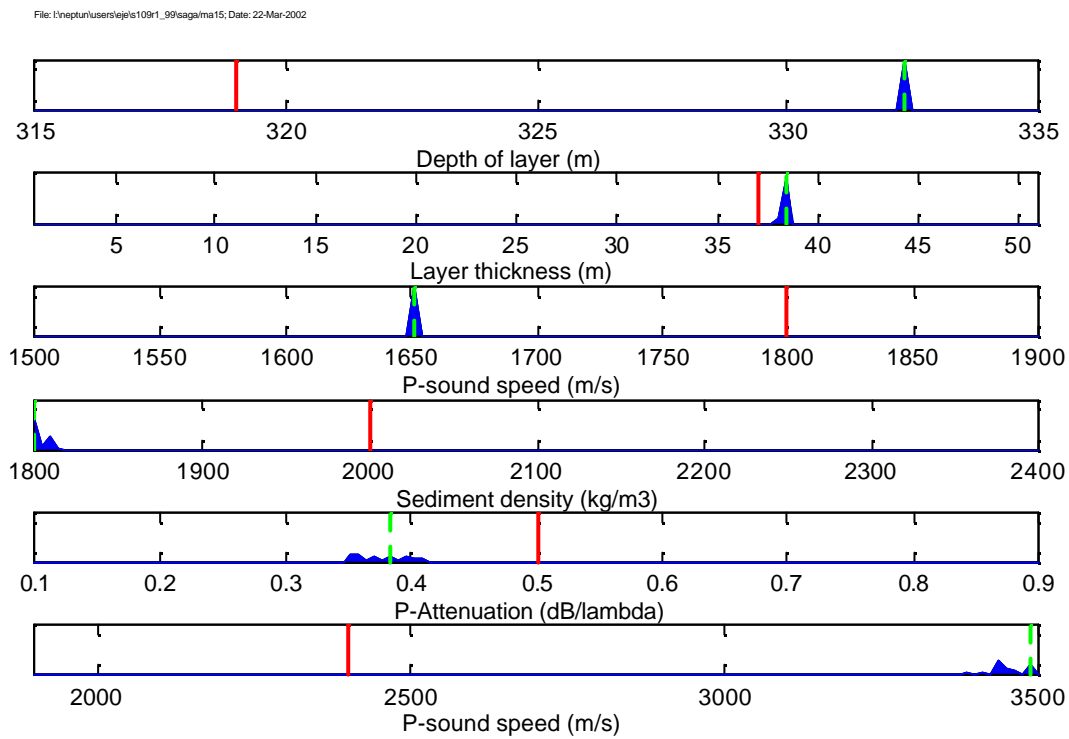


*Figure C.1* Inversion results for six parameters of shot # 109. Multi-frequency, 15 frequencies in three bands centred at 41.0 Hz, 48.6 Hz and 56.4 Hz. High SNR. SA GA parameters: 3000/64/6. Green, dotted line: GA best estimates. Red, solid line: GA baseline estimates.

File: l:\neptun\users\leje\l110r1\_99\saga\ma15; Date: 22-Mar-2002

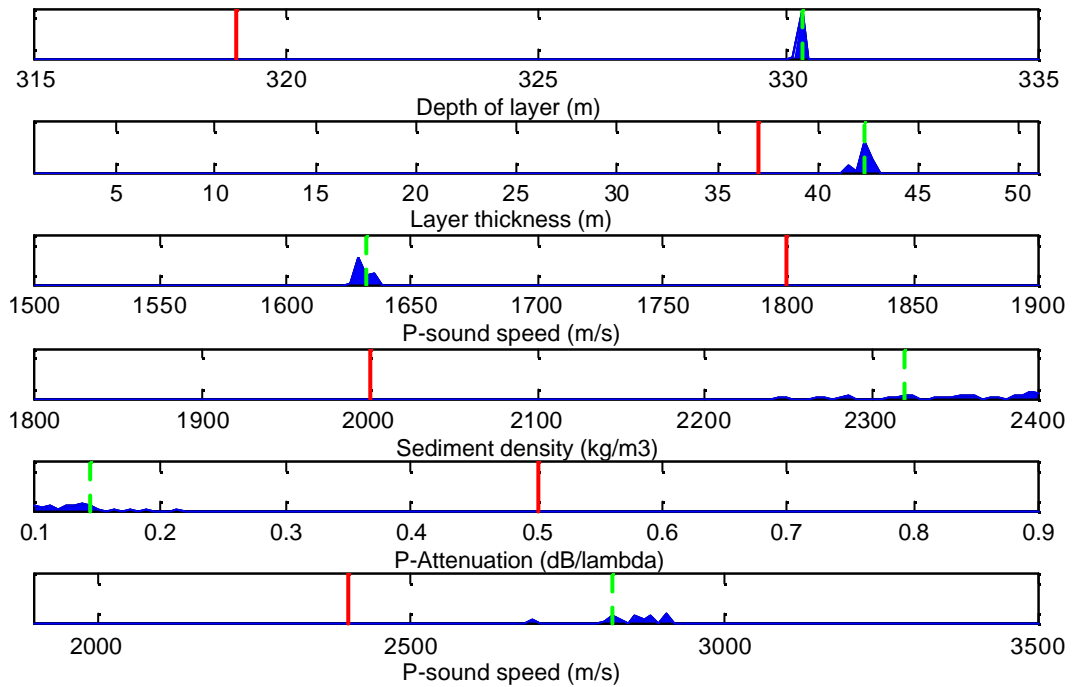


*Figure C.2 Inversion results for six parameters of shot # 110. Multi-frequency, 15 frequencies in three bands centred at 44.3 Hz, 53.7 Hz and 75.1 Hz. High SNR. SA GA parameters: 3000/64/6. Green, dotted line: GA best estimates. Red, solid line: GA baseline estimates.*

File: l:\neptun\users\leje\l111r1\_99\saga\ma15; Date: 22-Mar-2002

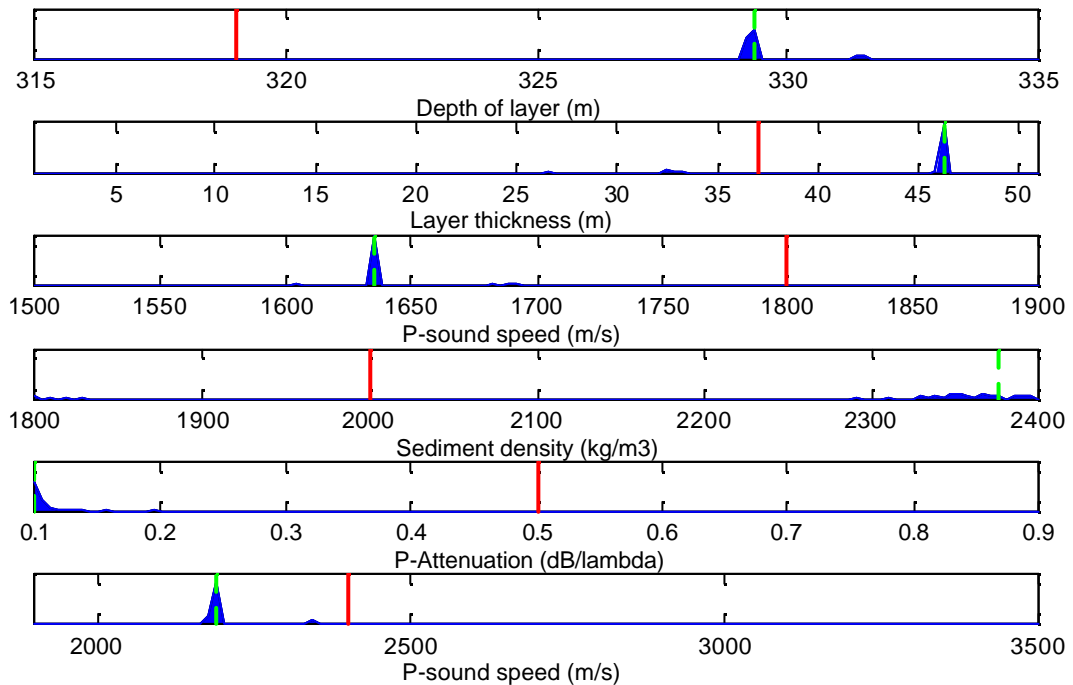


*Figure C.3 Inversion results for six parameters of shot # 111. Multi-frequency, 15 frequencies in three bands centred at 49.5 Hz, 60.5 Hz and 94.4 Hz. High SNR. SA GA parameters: 3000/64/6. Green, dotted line: GA best estimates. Red, solid line: GA baseline estimates.*

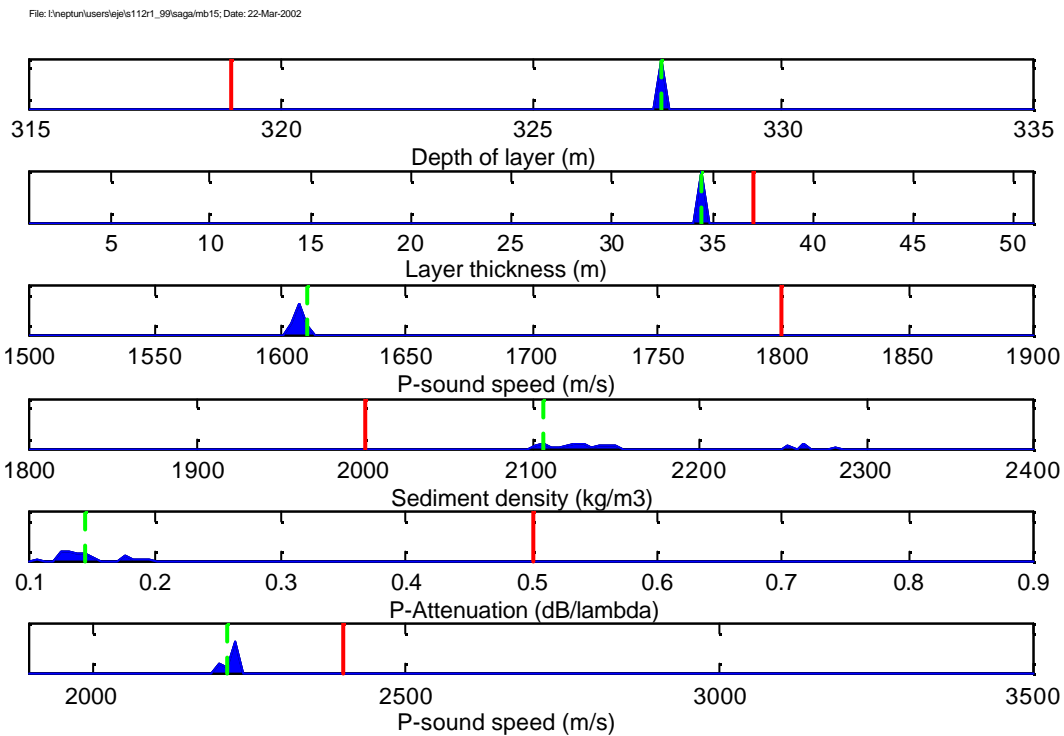


**Figure C.4** Inversion results for six parameters of shot # 112. Multi-frequency, 15 frequencies in three bands. SA GA parameters: 3000/64/6. Green, dotted line: GA best estimates. Red, solid line: GA baseline estimates.

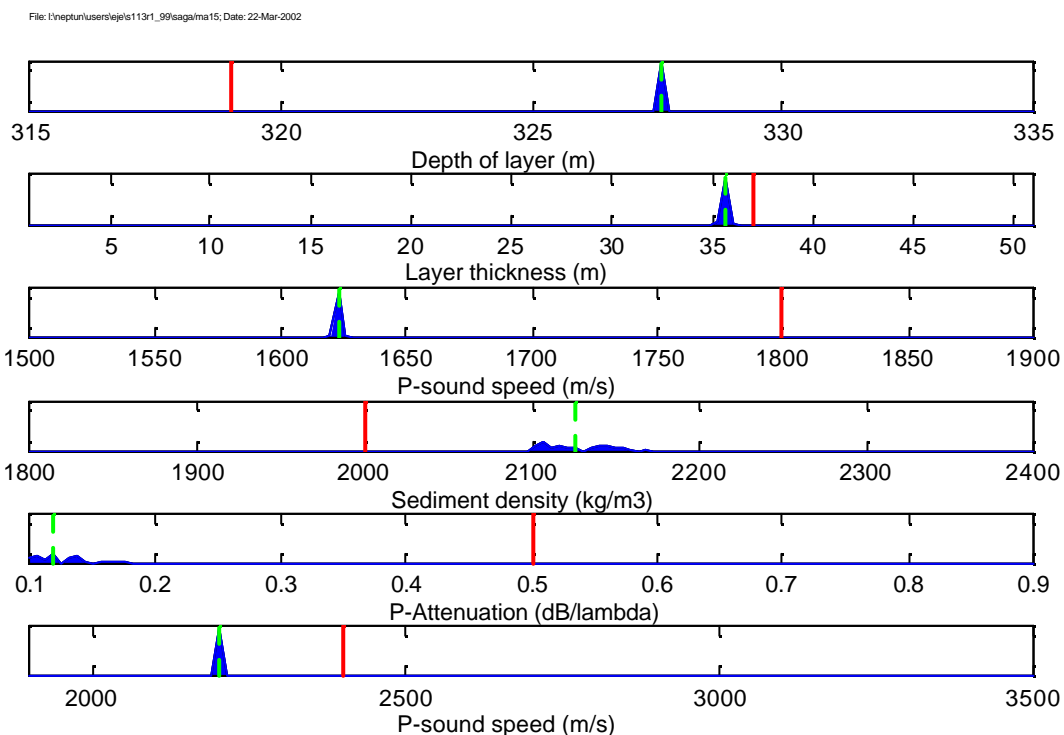


**Figure C.5** Inversion results for six parameters of shot # 113. Multi-frequency, 15 frequencies in three bands centred at 44.3 Hz, 53.7 Hz and 75.1 Hz. High SNR. SA GA parameters: 3000/64/6. Green, dotted line: GA best estimates. Red, solid line: GA baseline estimates.

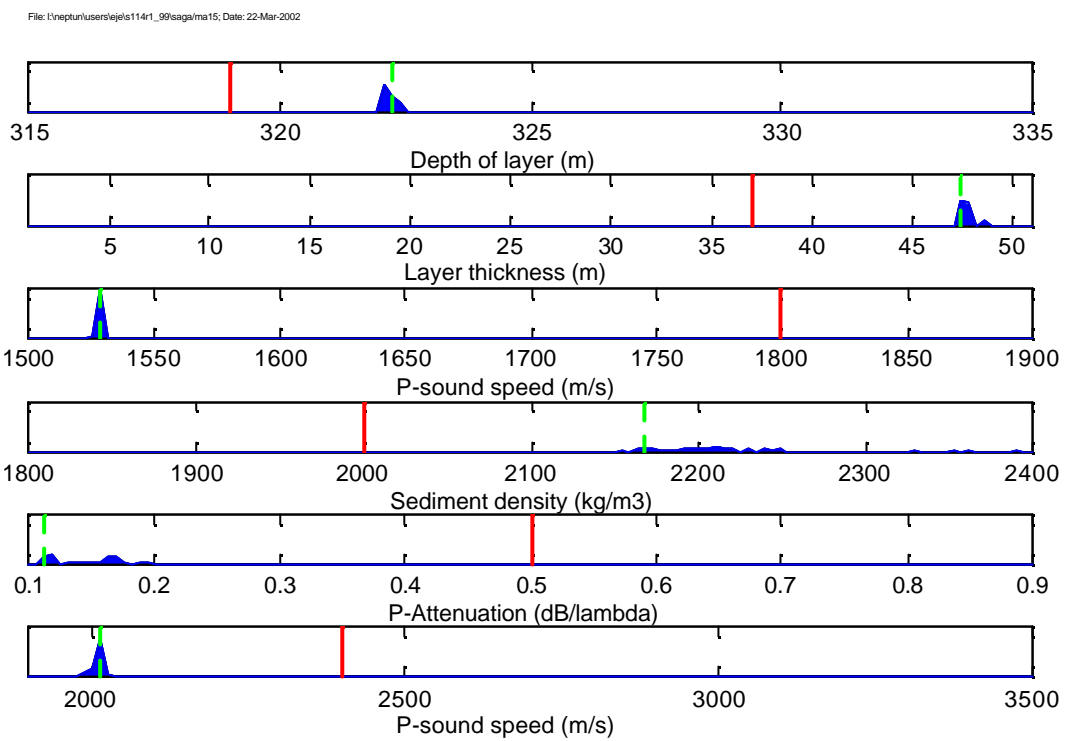


*Figure C.6 Inversion results for six parameters of shot # 114. Multi-frequency, 15 frequencies in three bands centred at 49.5 Hz, 60.5 Hz and 94.4 Hz. High SNR. SA GA parameters: 3000/64/6. Green, dotted line: GA best estimates. Red, solid line: GA baseline estimates.*

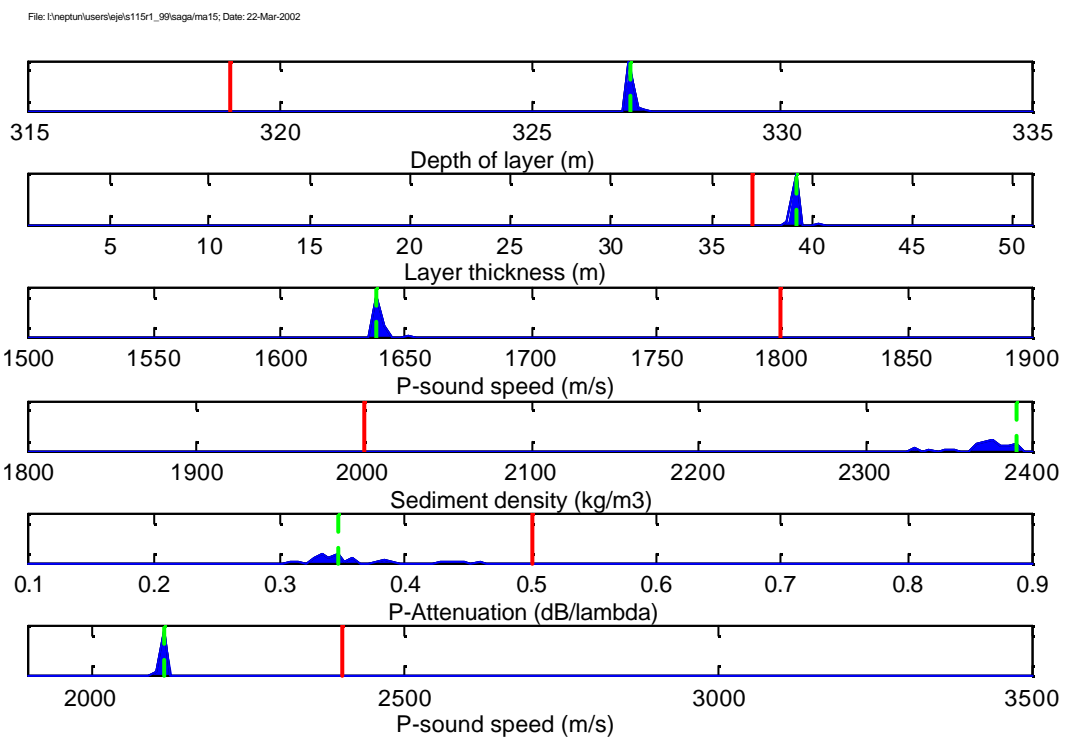


*Figure C.7 Inversion results for six parameters of shot # 115. Multi-frequency, 15 frequencies in three bands centred at 41.0 Hz, 48.6 Hz and 56.4 Hz. High SNR. SA GA parameters: 3000/64/6. Green, dotted line: GA best estimates. Red, solid line: GA baseline estimates.*

## D A POSTERIORI DISTRIBUTIONS FROM SOURCE LOCALIZATION

The *a posteriori* probability distributions from source localizations of the shots # 109 - # 115 are plotted in the below figures. The best model is marked as green, dashed lines, while the baseline model is marked as red, solid lines.

Three geoacoustic models were used as input:

- BM: Baseline model, inverting source depth and range
  - M2: Modified model, inverting source depth and range
  - M3: Modified model, inverting source depth and range, in addition to the water depth

The modified model had sediment velocity 1600 m/s instead of 1800 m/s as in the baseline model, and sediment attenuation 0.15 dB/λ instead of 0.5 dB/λ.

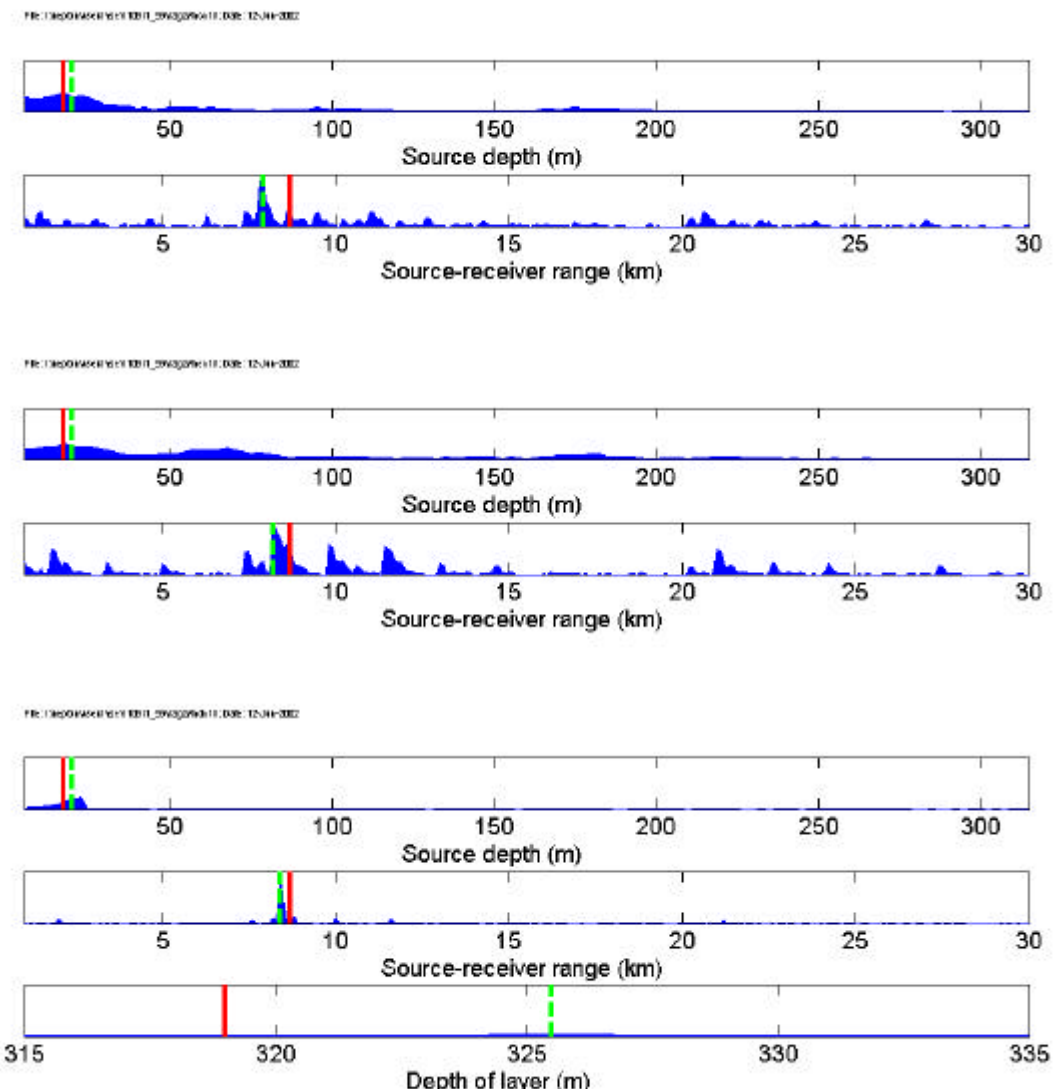
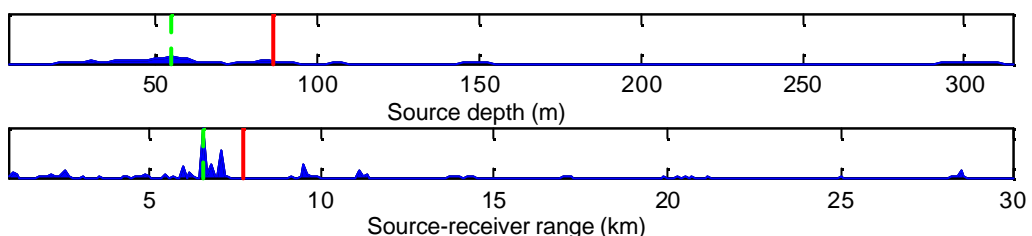
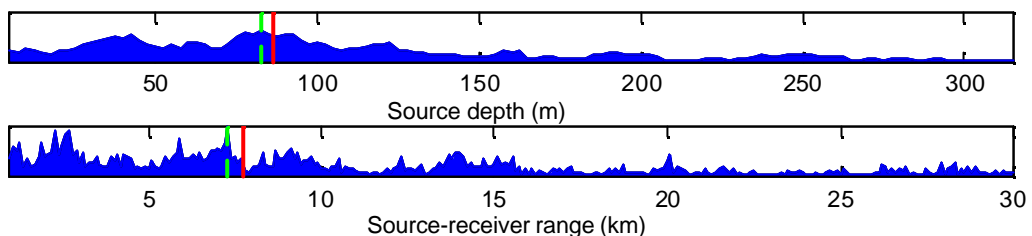


*Figure D.1 Source localization of shot # 109 S. Upper: Baseline model. Middle: Modified baseline model. Lower: Modified baseline model, inverting water depth. True range 8.70 km. True source depth 17.3 m.*

File: \neptun\users\jeje\s110r1\_99saga\mcn15; Date: 27-May-2002



File: \neptun\users\jeje\s110r1\_99saga\mdn15; Date: 27-May-2002



File: \neptun\users\jeje\s110r1\_99saga\men15; Date: 27-May-2002

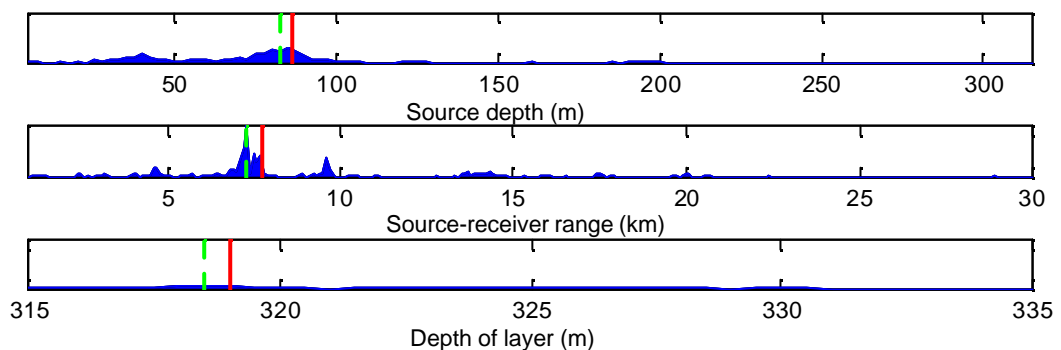
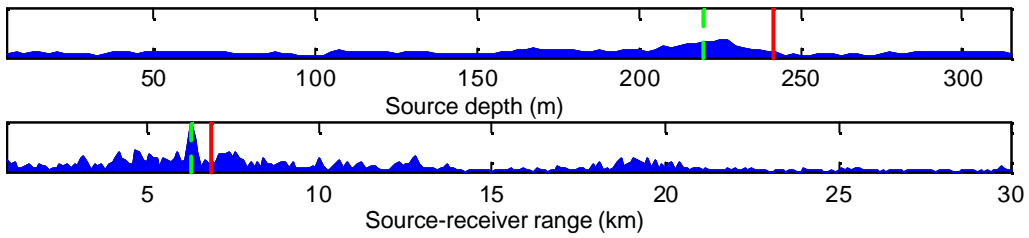
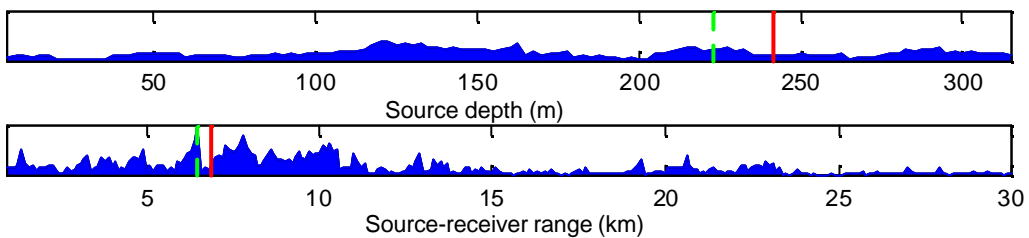


*Figure D.2* Source localization of shot # 110 I. Upper: Baseline model. Middle: Modified baseline model. Lower: Modified baseline model, inverting water depth. True range 7.76 km. True source depth 86.2 m.

File: l:\neptun\users\leje\ls111r1\_99\saga\mcn215; Date: 27-May-2002



File: l:\neptun\users\leje\ls111r1\_99\saga\mer215; Date: 27-May-2002



File: l:\neptun\users\leje\ls111r1\_99\saga\mdn215; Date: 27-May-2002

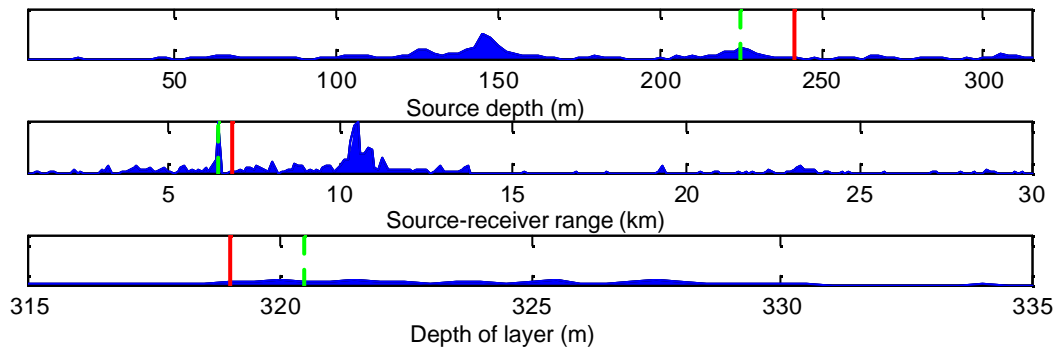


*Figure D.3* Source localization of shot # 111 D. Upper: Baseline model. Middle: Modified baseline model. Lower: Modified baseline model, inverting water depth. True range 6.83 km. True source depth 241.4 m.

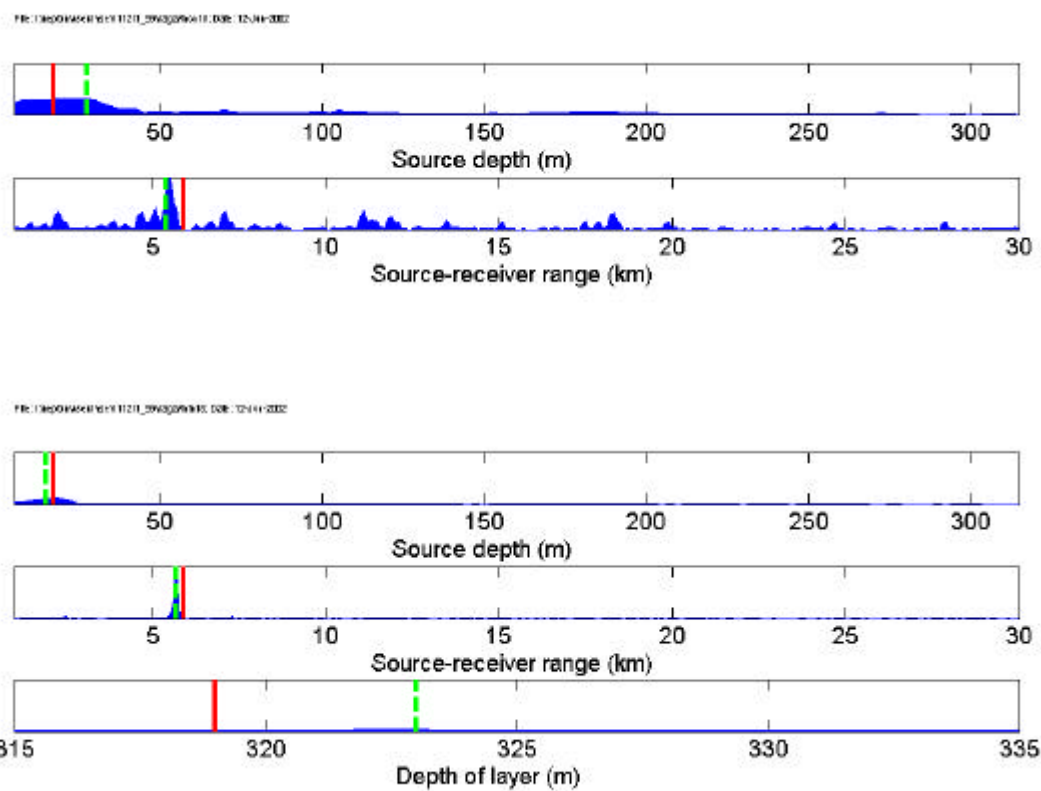


*Figure D.4* Source localization of shot # 112 S. Upper: Baseline model. Lower: Modified baseline model, inverting water depth. True range 5.91 km. True source depth 17.2 m.

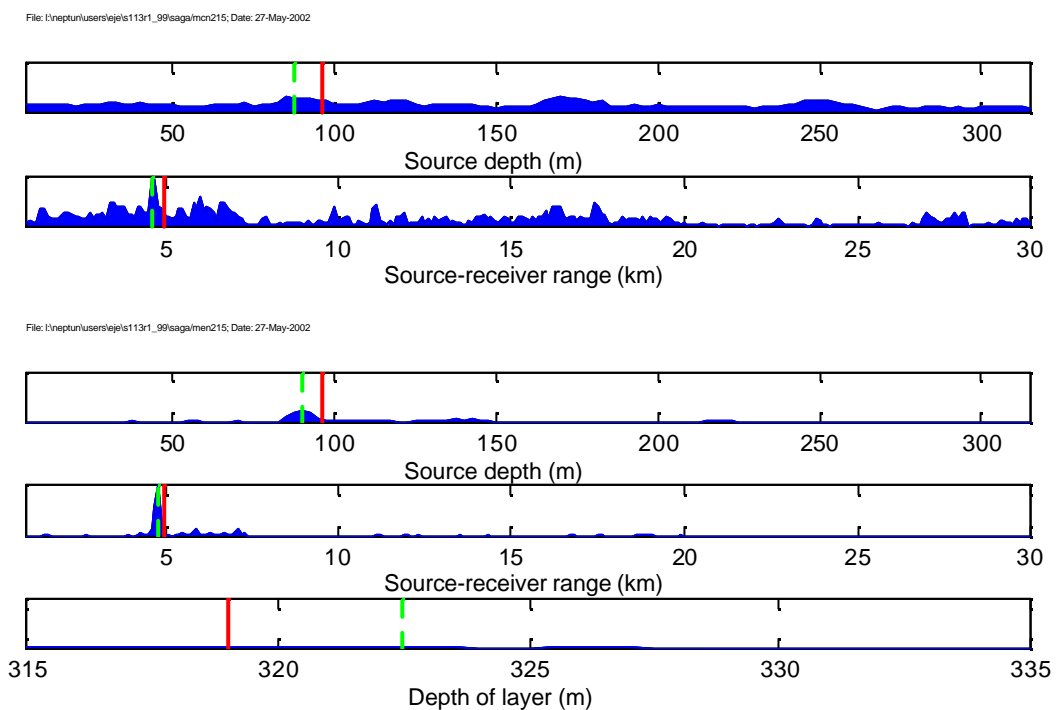


*Figure D.5* Source localization of shot # 113 I. Upper: Baseline model. Lower: Modified baseline model, inverting water depth. True range 4.98 km. True source depth 96.1 m.

File: I:\neptun\users\ejel\s114r1\_99\saga\mcn15; Date: 27-May-2002

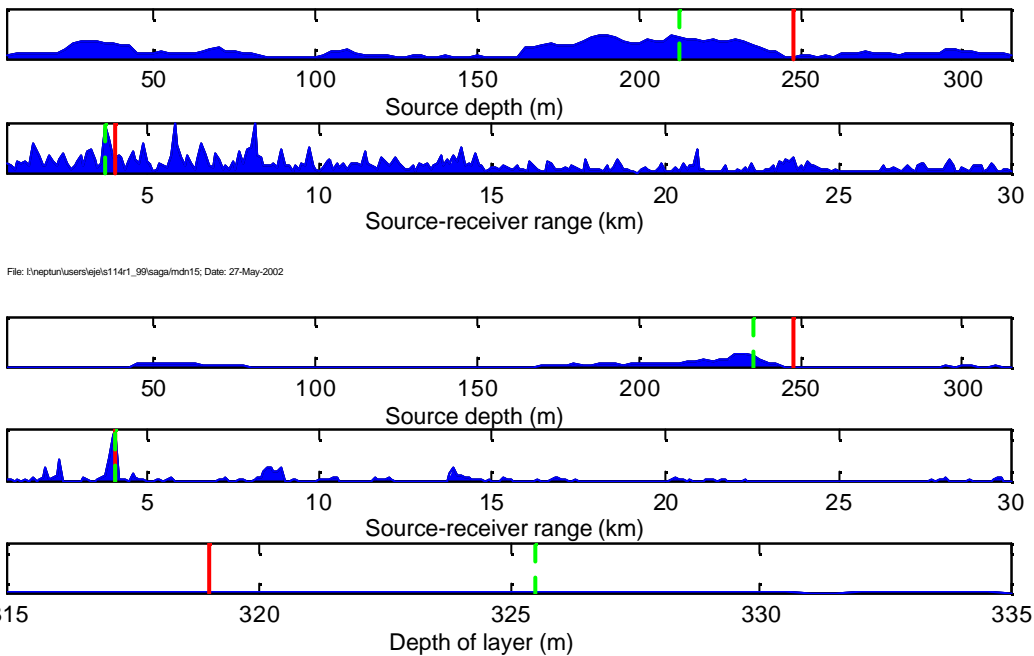


*Figure D.6 Source localization of shot # 114 D. Upper: Baseline model. Lower: Modified baseline model, inverting water depth. True range 4.07 km. True source depth 247.5 m.*

File: I:\neptun\users\ejel\s115r1\_99\saga\mdn15; Date: 27-May-2002

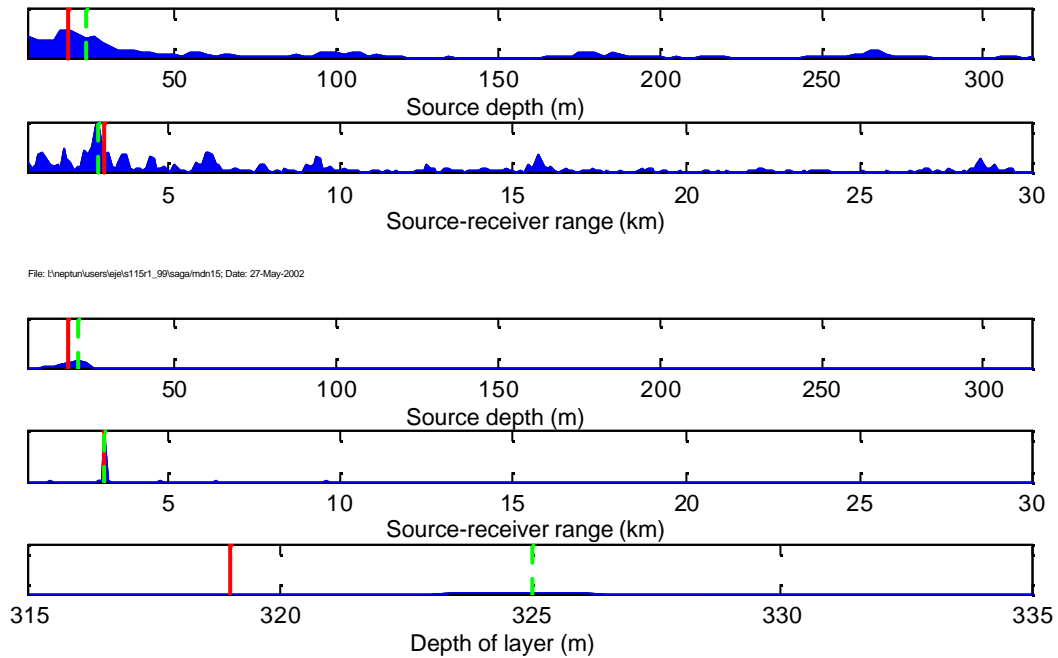


*Figure D.7 Source localization of shot # 115 S. Upper: Baseline model. Lower: Modified baseline model, inverting water depth. True range 3.17 km. True source depth 17.2 m.*

## References

- (1) Eidem E J, Bendiksen B, Helgesen H (1999): Project Swasi: Technical Cruise Report from Phase S-V 1999, FFI/RAPPORT-99/04955, Exempt from public disclosure
- (2) Johnsen J (1999): SWASI II - Cruise Report, Phase S-V 1999, FFI/NOTAT-99/05715, Exempt from public disclosure
- (3) Eidem E J (2001): Single Shot Inversion from the L-Antenna Experiment in 1999, FFI/RAPPORT-2001/02927
- (4) Eidem E J (2000): A 1040 m Deployable Hydrophone Array and its Data Acquisition System - Part II: Detailed description, FFI/RAPPORT-2000/04034, Exempt from public disclosure
- (5) Eidem E J (2000): A 1040 m Deployable Hydrophone Array and its Data Acquisition System - Part II: General description and data formats, FFI/RAPPORT-2000/04034, Exempt from public disclosure
- (6) Eidem E J (2000): Estimation of the Hydrophone Array Position During Swasi 1999 Phase S-V, FFI/RAPPORT-2000/04107, Exempt from public disclosure
- (7) Solberg C E (2001): Geoakustiske modeller for MFP eksperiment i Barentshavet august 1999, FFI/RAPPORT-2001/00335
- (8) Gerstoft P (1999): SAGA User Manual 3.0: An inversion software package, SACLANTCEN and Marine Physical Laboratory
- (9) Gerstoft P (2001): SAGA User Manual 4.1: An inversion software package, SACLANTCEN and Marine Physical Laboratory
- (10) Schmidt H (1999): OASES Version 2.1: User Guide and Reference Manual, Massachusetts Institute of Technology, USA.



# DISTRIBUTION LIST

**FFIBM****Dato:** 28. juni 2002

<b>RAPPORTTYPE (KRYSS AV)</b>	<b>RAPPORT NR.</b>	<b>REFERANSE</b>	<b>RAPPORTENS DATO</b>
<input checked="" type="checkbox"/> RAPP <input type="checkbox"/> NOTAT <input type="checkbox"/> RR	2002/02565	FFIBM/786/115	28. juni 2002
<b>RAPPORTENS BESKYTTELSESGRAD</b>		ANTALL EKS UTSTEDT	ANTALL SIDER
Unclassified		33	49
<b>RAPPORTENS TITTEL</b>  BROADBAND INVERSION AND SOURCE LOCALIZATION OF VERTICAL ARRAY DATA FROM THE L-ANTENNA EXPERIMENT IN 1999		<b>FORFATTER(E)</b>  EIDEM Ellen Johanne	
<b>FORDELING GODKJENT AV FORSKNINGSSJEF</b>  Jarl Johnsen		<b>FORDELING GODKJENT AV AVDELINGSSJEF:</b>  Jan Ivar Botnan	

**EKSTERN FORDELING****INTERN FORDELING**

ANTALL	EKS NR	TIL	ANTALL	EKS NR	TIL
1		FO/E	14		FFI-Bibl
1		Ved: Asgeir Berg	1		Adm direktør/stabssjef
1		NTNU Ved: Jens Hovem	1		FFIE
		7034 Trondheim	1		FFISYS
			1		FFIBM
			1		FFIN
			4		FFIBM/Horten
			1		Ellen J Eidem, FFIBM/Horten
			1		Trond Jenserud, FFIBM/Horten
			1		Connie E Solberg, FFIBM/Horten
			1		Torgeir Svolsbru, FFIBM/Horten
			1		Knut A Søstrand, FFIBM/Horten
			1		Dag TollefSEN, FFIBM/Horten
			1		Torgeir Svolsbru, FFIBM/Horten
			1		FFI-veven